

# Graph reduction by local variation

Andreas Loukas  
 École Polytechnique Fédérale Lausanne,  
 Switzerland

## Abstract

How can we reduce the size of a graph without significantly altering its basic properties? We approach the graph reduction problem from the perspective of restricted similarity, a modification of a well-known measure for graph approximation. Our choice is motivated by the observation that restricted similarity implies strong spectral guarantees and can be used to prove statements about certain unsupervised learning problems. The paper then focuses on coarsening—a popular type of graph reduction. We derive sufficient conditions for a small graph to approximate a larger one in the sense of restricted similarity. Our theoretical findings give rise to a novel quasi-linear algorithm. Compared to both standard and advanced graph reduction methods, the proposed algorithm finds coarse graphs of improved quality –often by a large margin– without sacrificing speed.

## 1 Introduction

As graphs grow in size it becomes pertinent to approximately solve graph learning problems within a reasonable computational budget. Typically this is pursued in a per-case basis, with significant research efforts devoted to accelerating each useful algorithm. Alternatively, we can look for ways to reduce the inherent problem difficulty by simplifying the graph in question, while making sure that we do not lose too much information.

There are two main ways to simplify graphs. First, one may reduce the number of edges, a technique commonly referred to as *graph sparsification*. Starting with the seminal work by Spielman and Teng [34], the idea is to remove and re-weight edges aiming to identify a sparse graph whose properties are appropriately similar to the original graph. Graph sparsification techniques can yield significant benefits whenever the number of edges is the computational bottleneck and have been used successfully to solve linear systems involving positive semi-definite matrices and graph-regularized inverse problems, among others.

Alternatively, one may seek to reduce directly the size of the graph, i.e., the number  $N$  of its vertices, by some form of vertex selection or re-combination scheme. This idea can be traced back to the multigrid literature, that targets the acceleration of finite-element methods using cycles of multilevel coarsening, lifting and refinement. After being generalized to graphs, reduction methods have become pervasive in computer science and form a key element of modern graph learning pipelines, both for unsupervised learning problems such as graph partitioning [16, 20, 23, 10, 40] and visualization [21, 18, 39], as well as for supervised learning tasks tackled with graph convolutional neural networks [3, 9, 2, 33]. Reduction methods have also been used to create multi-scale representations of graph-structured data [24, 14, 32], to solve linear systems [22, 26], to approximate the Fiedler vector [37, 13], and to accelerate least-squares problems [17, 7]. Some of their main benefits are the ability to deal with sparse graphs –graphs with at most  $O(N \log N)$

edges— and to accelerate algorithms whose complexity depends on the number of vertices as well as edges.

Yet, despite their popularity, to-date there has been only circumstantial theory supporting graph reduction methods [11, 27]. The lack of a concrete understanding of how different reduction choices affect fundamental graph properties (especially those relevant to learning problems) is an issue: there is currently no rigorous way to determine how (and how much) we can benefit from reduction.

**A new perspective.** Attempting to provide answers, this paper approaches graph reduction from the perspective of *similarity*, a key measure used in sparsification to judge how well a graph approximates another one. To render it applicable to graphs of different sizes, we restrict similarity over a subspace of size that is at most equal to the size of the reduced graph and refer to the resulting definition as *restricted similarity*. Despite being a statement about subspaces, restricted similarity has important consequences. It is shown that when the subspace in question is an eigenspace (this is a data agnostic choice where one wants to preserve the global graph structure), the eigenvalues and eigenspaces of the reduced graph approximate those of the original large graph. It is then a corollary that (i) if the large graph has a good cut so does the smaller one; and (ii) that unsupervised learning algorithms that utilize spectral embeddings, such as spectral clustering and Laplacian eigenmaps, can also work well when run on the smaller graph and their solution is lifted.

The paper then focuses on *graph coarsening*—a popular type of graph reduction where, in each level, reduced vertices are formed by contracting disjoint sets of connected vertices (each such set is called a *contraction set*). We derive sufficient conditions for a small coarse graph to approximate a larger graph in the sense of restricted similarity. Crucially, this result holds for any number of levels and is independent of how the subspace is chosen. Though the derived bound is involved, a decoupling argument renders it separable over contraction sets and can be interpreted as measuring the *local variation* over each contraction set (it involves the maximum variation of vectors supported on each induced subgraph).

These findings give rise to a novel quasi-linear algorithm for graph coarsening. The algorithm starts from a family of candidate contraction sets. Even though any connected set of vertices may form a valid candidate set, following common wisdom we opt for small well-connected sets, formed for example by pairs of adjacent vertices or neighborhoods. It then iteratively contracts those sets whose local variation is the smallest. Depending on how the contraction family is constructed we obtain different solutions, trading off computational complexity for reduction.

**Theoretical and practical implications.** Our analysis improves and generalizes upon previous works in a number of ways:

- Instead of directly focusing on specific constructions, we study a general graph reduction scheme featuring coarsening as a special case. As a consequence, the implications of restricted similarity are proven in a fairly general setting where specifics of the reduction (such as the type of graph representation and the reduction matrices involved) are abstracted.
- Contrary to previous results, our analysis holds for multiple levels of reduction. Given that the majority of coarsening methods reduce the number of vertices by a constant factor at each level, a multilevel approach is necessary to achieve significant reduction. Along that line, our analysis also brings an arguably intuitive insight: rather than taking the common approach of approximating at each level the graph produced by the previous level, one should strive to preserve the properties of the original graph at every level.
- The proposed algorithm is not heuristically designed but follows from a relaxation of the

restricted similarity objective. Despite the breadth of the literature that utilizes some form of graph reduction, the overwhelming majority of known methods are heuristics—see for instance [31]. A notable exception is Kron reduction [11], an elegant method that aims to preserve the effective resistance distance. Compared to Kron reduction, local variation methods are accompanied by significantly stronger spectral guarantees (i.e., beyond interlacing), do not sacrifice the sparsity of the graph, and are ultimately more scalable as they do not rely on the Schur complement of the Laplacian.

To demonstrate the practical benefits of our approach, we complement our analysis with numerical results on representative graphs ranging from scale-free graphs to meshes and road networks. Compared to both standard [20] and advanced reduction methods [30, 26, 32], local variation methods yield small graphs of improved quality, often by a large margin, without being much slower than naive heavy-edge matching. A case in point, when examining how close are the principal eigenvalues of the coarse and original graph for a reduction of 70%, local variation methods attain on average  $2.6\times$  smaller error; this gain becomes  $3.9\times$  if we don't include Kron reduction in the comparison.

## 2 Graph reduction and coarsening

The following section introduces graph reduction from a linear algebraic perspective. Our exposition starts by considering a general graph reduction scheme. We then show how graph coarsening arises naturally if we additionally impose requirements w.r.t. the interpretability of reduced variables.

### 2.1 Graph reduction

Consider a positive semidefinite (PSD) matrix  $L \in \mathbb{R}^{N \times N}$  whose sparsity structure captures the connectivity structure of a connected weighted symmetric graph  $G = (\mathcal{V}, \mathcal{E}, W)$  of  $N = |\mathcal{V}|$  vertices and  $M = |\mathcal{E}|$  edges. In other words,  $L(i, j) \neq 0$  only if  $e_{ij}$  is a valid edge. Moreover, let  $x$  be an arbitrary vector of size  $N$ .

We study the following generic reduction scheme:

#### Scheme 1: Graph reduction

Commence by setting  $L_0 = L$  and  $x_0 = x$  and proceed according to the following two recursive equations:

$$L_\ell = P_\ell^\mp L_{\ell-1} P_\ell^+ \quad \text{and} \quad x_\ell = P_\ell x_{\ell-1},$$

where  $P_\ell \in \mathbb{R}^{N_\ell \times N_{\ell-1}}$  are matrices with more columns than rows,  $\ell = 1, 2, \dots, c$  is the level of the reduction, symbol  $\mp$  denotes the transposed pseudoinverse, and  $N_\ell$  is the dimensionality at level  $\ell$  such that  $N_0 = N$  and  $N_c = n \ll N$ .

Vector  $x_c$  is lifted back to  $\mathbb{R}^N$  by recursion  $\tilde{x}_{\ell-1} = P_\ell^+ \tilde{x}_\ell$ , where  $\tilde{x}_c = x_c$ .

Graph reduction thus involves a sequence of  $c + 1$  graphs

$$G = G_0 = (\mathcal{V}_0, \mathcal{E}_0, W_0) \quad G_1 = (\mathcal{V}_1, \mathcal{E}_1, W_1) \quad \dots \quad G_c = (\mathcal{V}_c, \mathcal{E}_c, W_c) \quad (1)$$

of decreasing size  $N = N_0 > N_1 > \dots > N_c = n$ , where the sparsity structure of  $L_\ell$  matches that of graph  $G_\ell$ , and each vertex of  $G_\ell$  represents one of more vertices of  $G_{\ell-1}$ .

The multilevel design allows us to achieve high dimensionality reduction, even when at each level the *dimensionality reduction ratio*

$$r_\ell = 1 - \frac{N_\ell}{N_{\ell-1}}$$

is small. For instance, supposing that  $r_\ell \geq \varrho$  for each  $\ell$ , then  $c = O(\log(n/N)/\log(1 - \varrho))$  levels suffice to reduce the dimension to  $n$ .

We can express the reduced quantities in a more compact form:

$$x_c = Px, \quad L_c = P^\top LP^+ \quad \text{and} \quad \tilde{x} = \Pi x, \quad (2)$$

where  $P = P_c \cdots P_1$ ,  $P^+ = P_1^+ \cdots P_c^+$ , and  $\Pi = P^+P$ . For convenience, we drop zero indices and refer to a lifted vector as  $\tilde{x} (= \tilde{x}_0)$ .

The rational of this scheme is that vector  $\tilde{x}$  should be the best approximation of  $x$  given  $P$  in an  $\ell_2$ -sense, which is a consequence of the following property:

**Property 2.1.**  $\Pi$  is a projection matrix.

On the other hand, our matrix  $L$  is reduced such that  $x_c^\top L_c x_c = \tilde{x}^\top L \tilde{x}$ .

## 2.2 Properties of reduced graphs

Even in this general context, where  $P$  is an arbitrary  $n \times N$  matrix, certain handy properties can be proven about the relation between  $L_c$  and  $L$ .

To begin with, it is simple to see that the set of positive semidefinite matrices is closed under reduction.

**Property 2.2.** If  $L$  is PSD, then so is  $L_c$ .

The proof is elementary: if  $L$  is PSD then there exists matrix  $S$  such that  $L = S^\top S$ , implying that  $L_c = P^\top LP^+$  can also be written as  $L_c = S_c^\top S_c$  if we set  $S_c = SP^+$ .

We further consider the spectrum of the two matrices. We sort the eigenvalues of  $L$  as  $\lambda_1 \leq \lambda_2 \leq \dots \leq \lambda_N$  and denote by  $\lambda_k$  the  $k$ -th largest eigenvalue of  $L_c$  and  $\tilde{u}_k$  the associated eigenvector.

In addition, the eigenvalues  $\tilde{\lambda}$  and  $\lambda$  are interlaced.

**Theorem 2.3.** The interlacing inequality  $\lambda_k \leq \tilde{\lambda}_k \leq \lambda_{k+N-n}$  holds for all  $k = 1, \dots, n$ .

This result is a generalization of the interlacing inequalities known for the normalized Laplacian. Chen et al. [4] showed in Theorem 2.7 of their paper that after contracting  $N - n$  edges  $\lambda_{k-N+n} \leq \lambda_k \leq \lambda_{k+N-n}$  for  $k = 1, 2, \dots, n$  and with  $\lambda_\ell = 0$  when  $\ell \leq 0$ , matching our upper bound. Our lower bound is matched in [6, Lemma 1.15], again derived for the normalized Laplacian. Also notably, the inequalities match those known for Kron reduction [11, Lemma 3.6].

Theorem 2.3 is particularly pessimistic as it has to hold for every possible  $P$  and  $L$ . We will obtain much stronger results later on by restricting our attention to constructions that satisfy additional properties (see Theorem 3.3).

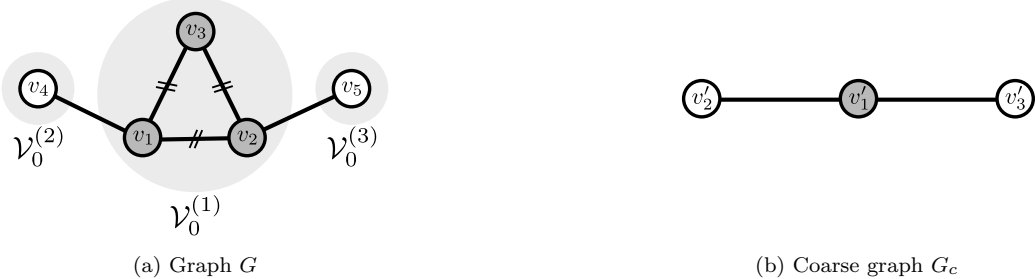


Figure 1: Toy coarsening example. Grey discs denote contraction sets. The first three vertices of  $G$  forming contraction set  $\mathcal{V}_0^1$  are contracted onto vertex  $v'_1$ . All other vertices remain unaffected.

We can also say something about the eigenvectors. It is simple to deduce that for every vector for which  $x = \Pi x$ , we have

$$x_c^\top L_c x_c = x^\top \Pi L \Pi x = x^\top L x \quad \text{and} \quad \tilde{x} = \Pi x = x.$$

In other words, reduction maintains the action of  $L$  of every vector that lies in the range of  $\Pi$ . Naturally, after lifting the eigenvectors  $\tilde{u}_k$  of  $L_c$  are included in this class.

### 2.3 Coarsening as a type of graph reduction

In contrast to graph reduction, in coarsening matrices  $P_1, P_2, \dots, P_c$  are not arbitrary, but abide to a few constraints that render the graph transformation interpretable.

More precisely, in coarsening one selects for each level  $\ell$  a surjective map  $\varphi_\ell : \mathcal{V}_{\ell-1} \rightarrow \mathcal{V}_\ell$  between the original vertex set  $\mathcal{V}_{\ell-1}$  and the smaller vertex set  $\mathcal{V}_\ell$ . We refer to the set of vertices  $\mathcal{V}_{\ell-1}^{(r)} \subseteq \mathcal{V}_{\ell-1}$  mapped onto the same vertex  $v'_r$  of  $\mathcal{V}_\ell$  as a *contraction set*:

$$\mathcal{V}_{\ell-1}^{(r)} = \{v \in \mathcal{V}_{\ell-1} : \varphi_\ell(v) = v'_r\}$$

For a graphical depiction of contraction sets, see Figure 1. We then constrain  $\varphi_\ell$  slightly by requiring that the subgraph of  $G_{\ell-1}$  induced by each contraction set  $\mathcal{V}_{\ell-1}^{(r)}$  is connected.

It is easy to deduce from the above definition that contraction sets induce a partitioning of  $\mathcal{V}_{\ell-1}$  into  $N_\ell$  subgraphs, each corresponding to a single vertex of  $\mathcal{V}_\ell$ . Every reduced variable thus corresponds to a small set of adjacent vertices in the original graph and coarsening basically amounts to a scaling operation. An appropriately constructed coarse graph then aims to capture the global problem structure and neglected details can then be recovered in a local refinement phase.

We can place coarsening in the context of reduction scheme 1 by restricting each  $P_\ell$  to lie in the family of coarsening matrices, defined next:

**Definition 2.4** (Coarsening matrix). *Matrix  $P_\ell \in \mathbb{R}^{N_\ell \times N_{\ell-1}}$  is a coarsening matrix w.r.t. graph  $G_{\ell-1}$  if and only if it satisfies the following two conditions:*

- It is locality preserving. Equivalently, level  $\ell$  only entails the coarsening of vertices  $v_i, v_j$  for which  $e_{ij} \in \mathcal{E}_{\ell-1}$ .*
- It is a surjective mapping of the vertex set. Equivalently,  $P_\ell$ 's rows have disjoint support meaning that if  $P_\ell(r, i) \neq 0$  then there does not exist  $i' \neq i$  such that  $P_\ell(r, i') \neq 0$ .*

An interesting consequence of this definition is that, in contrast to graph reduction, with coarsening matrices the expensive pseudo-inverse computation can be substituted by simple transposition and re-scaling:

**Lemma 2.5** (Easy inversion). *The pseudo-inverse of a coarsening matrix  $P_\ell$  is given by  $P_\ell^+ = P_\ell^\top D_\ell^{-2}$ , where  $D_\ell$  is the diagonal matrix with  $D_\ell(r, r) = \|P_\ell(r, :)\|_2$ .*

This has two consequences. First, coarsening can be done very efficiently. Each coarsening level (both in the forward and backward directions) entails multiplication by a sparse matrix. This can be done very efficiently—both  $P_\ell$  and  $P_\ell^+$  have only  $N_{\ell-1}$  non-zero entries meaning that  $O(N)$  and  $O(M)$  computational operations suffice to coarsen respectively a vector and a matrix  $L$  whose sparsity structure reflects the graph adjacency. In addition, the number of graph edges also decreases at each level and quick calculations reveal that the coarser graph has in the worst case at most  $m = M - (N - n)$  edges (in practice,  $m$  can be significantly smaller).

## 2.4 Laplacian consistency

A further restriction that we can impose is that coarsening is consistent w.r.t. the Laplacian form. Let  $L$  be the combinatorial Laplacian of  $G$  defined as

$$L(i, j) = \begin{cases} d_i & \text{if } i = j \\ -w_{ij} & \text{if } e_{ij} \in \mathcal{E} \\ 0 & \text{otherwise,} \end{cases}$$

where  $w_{ij}$  is the weight associated with edge  $e_{ij}$  and  $d_i$  the weighted degree of  $v_i$ . We can prove the following lemma:

**Lemma 2.6** (Consistency). *Let  $P$  be a coarsening matrix w.r.t. a graph with combinatorial Laplacian  $L$ . Matrix  $L_c = P^\top L P^+$  is a combinatorial Laplacian if and only if the non-zero entries of  $P^+$  are equally valued.*

It is a corollary of Lemmas 2.5 and 2.6 that in a consistent coarsening scheme and for any  $v'_r \in \mathcal{V}_\ell$  and  $v_i \in \mathcal{V}_{\ell-1}$ , matrices  $P_\ell \in \mathbb{R}^{N_\ell \times N_{\ell-1}}$  and  $P_\ell^+ \in \mathbb{R}^{N_{\ell-1} \times N_\ell}$  should be given by:

$$P_\ell(r, i) = \begin{cases} \frac{1}{|\mathcal{V}_{\ell-1}^{(r)}|} & \text{if } v_i \in \mathcal{V}_{\ell-1}^{(r)} \\ 0 & \text{otherwise} \end{cases} \quad \text{and} \quad [P_\ell^+](i, r) = \begin{cases} 1 & \text{if } v_i \in \mathcal{V}_{\ell-1}^{(r)} \\ 0 & \text{otherwise,} \end{cases}$$

where the contraction sets  $\mathcal{V}_{\ell-1}^{(1)}, \dots, \mathcal{V}_{\ell-1}^{(N_\ell)}$  are defined in Section 2.3.

The toy graph shown in Figure 1a illustrates an example where the gray vertices  $\mathcal{V}_0^{(1)} = \{v_1, v_2, v_3\}$  of  $G$  are coarsened into vertex  $v'_1$ , as shown in Figure 1b. The main matrices we have defined are

$$P_1 = \begin{bmatrix} 1/3 & 1/3 & 1/3 & 0 & 0 \\ 0 & 0 & 0 & 1 & 0 \\ 0 & 0 & 0 & 0 & 1 \end{bmatrix} \quad P_1^+ = \begin{bmatrix} 1 & 0 & 0 \\ 1 & 0 & 0 \\ 1 & 0 & 0 \\ 0 & 1 & 0 \\ 0 & 0 & 1 \end{bmatrix} \quad \Pi = P_1^+ P_1 = \begin{bmatrix} 1/3 & 1/3 & 1/3 & 0 & 0 \\ 1/3 & 1/3 & 1/3 & 0 & 0 \\ 1/3 & 1/3 & 1/3 & 0 & 0 \\ 0 & 0 & 0 & 1 & 0 \\ 0 & 0 & 0 & 0 & 1 \end{bmatrix}$$

and coarsening results in

$$L_c = P_1^\top L P_1^+ = \begin{bmatrix} 2 & -1 & -1 \\ -1 & 1 & 0 \\ -1 & 0 & 1 \end{bmatrix} \quad x_c = P_1 x = \begin{bmatrix} (x(1) + x(2) + x(3))/3 \\ x(4) \\ x(5) \end{bmatrix}.$$

Finally, when lifted  $x_c$  becomes

$$\tilde{x} = P_1^+ x_c = \begin{bmatrix} (x(1) + x(2) + x(3))/3 \\ (x(1) + x(2) + x(3))/3 \\ (x(1) + x(2) + x(3))/3 \\ x(4) \\ x(5) \end{bmatrix}.$$

Since vertices  $v_4$  and  $v_5$  are not coarsened, the respective contraction sets  $\mathcal{V}_0^{(2)}$  and  $\mathcal{V}_0^{(3)}$  are singleton sets.

In general, the weight  $W_1(r, q)$  between vertices  $v'_r$  and  $v'_q$  in level 1 is equal to the sum of all weights going from a vertex in the contraction set  $\mathcal{V}_0^{(r)}$  to a vertex in  $\mathcal{V}_0^{(q)}$ :

$$W_1(r, q) = \sum_{v_i \in \mathcal{V}_0^{(r)}, v_j \in \mathcal{V}_0^{(q)}} w_{ij}.$$

In our example there is a single edge of unit weight connecting vertices in  $\mathcal{V}_0^{(1)}$  and  $\mathcal{V}_0^{(2)}$  and as such the weight between  $v'_1$  and  $v'_2$  is equal to one.

Finally, as is desirable, the structure of the nullspace of  $L$  is preserved both by coarsening and lifting:

$$P_1 1_N = 1_n \quad \text{and} \quad P_1^+ 1_n = 1_N,$$

where the subscript indicates dimensionality.

### 3 Algebraic measures of reduction quality

This section aims to formalize how should a graph be reduced such that the structure of the reduced and original problems should be as close as possible. Inspired by work in numerical linear algebra, we introduce a measure of similarity that is tailored to graph reduction. Our definition implies strong guarantees about the similarity of the original and coarsened spectrum.

The insights presented here will be exploited in Section 4 in order to design efficient graph coarsening algorithms.

#### 3.1 Restricted graph similarity

One way to define how close a PSD matrix  $L$  is to its reduced counterpart is to establish an isometry guarantee w.r.t. the following induced semi-norms:

$$\|x\|_L = \sqrt{x^\top L x} \quad \text{and} \quad \|x_c\|_{L_c} = \sqrt{x_c^\top L_c x_c}$$

Ideally, we would hope that

$$(1 - \epsilon) \|x\|_L \leq \|x_c\|_{L_c} \leq (1 + \epsilon) \|x\|_L \tag{3}$$

for all  $x \in \mathbb{R}^N$ .

If the equation holds, we say that matrices  $L_c$  and  $L$  are  $\epsilon$ -similar. The objective of constructing sparse similar graphs is the main idea of spectral graph sparsifiers, a popular method for accelerating the solution of linear systems involving the Laplacian [34].

In contrast to graph sparsification however, since here the dimension of the space changes it is impossible to satisfy (3) for every  $x \in \mathbb{R}^N$  (this follows by a simple rank argument). To carry out a meaningful analysis, we need to consider a subspace of dimension  $k \leq n$ .

We can then define a (subspace) restricted notion of matrix similarity:

**Definition 3.1** (Restricted similarity). *Let  $\mathcal{R}$  be a  $k$ -dimensional subspace of  $\mathbb{R}^N$  such that  $k \leq n \leq N$ . Matrices  $L_c$  and  $L$  are  $(\mathcal{R}, \epsilon)$ -similar if there exists an  $\epsilon \geq 0$  such that*

$$(1 - \epsilon) \|x\|_L \leq \|x_c\|_{L_c} \leq (1 + \epsilon) \|x\|_L$$

for all  $x \in \mathcal{R}$ .

Clearly, if  $L_c$  and  $L$  are  $(\mathcal{R}, \epsilon)$ -similar then they are also  $(\mathcal{R}', \epsilon')$ -similar, where  $\mathcal{R}'$  is any subspace of  $\mathcal{R}$  and  $\epsilon' \geq \epsilon$ . As such, similarity statements about large subspaces and small  $\epsilon$  are the most desirable.

As we will see in Theorem 3.2, guaranteeing restricted similarity w.r.t. subspace  $\mathcal{R}$  boils down to minimizing at each level  $\ell$  the spectral norm

$$\|\Pi_\ell^\perp A_{\ell-1}\|_{L_{\ell-1}} = \|S_{\ell-1} \Pi_\ell^\perp A_{\ell-1}\|_2,$$

where  $S_{\ell-1}$  is the square-root of the PSD matrix  $L_{\ell-1}$  and  $\Pi_\ell^\perp = I - P_\ell^+ P_\ell$  is the complement projection matrix involved with  $P_\ell$ . Matrix  $A_{\ell-1}$  captures two types of information:

1. Foremost, it encodes the behavior of the target matrix  $L$  w.r.t.  $\mathcal{R}$ . This is clearly seen in the first level, for which we have that  $A_0 = VV^\top L^{+1/2}$  with  $V \in \mathbb{R}^{N \times k}$  being an orthonormal basis of  $\mathcal{R}$ .
2. When  $\ell > 1$  one needs to consider  $A_0$  in view of the reduction done in previous levels. The necessary modification turns out to be  $A_{\ell-1} = B_{\ell-1} (B_{\ell-1}^\top L_{\ell-1} B_{\ell-1})^{+1/2}$ , with  $B_{\ell-1} = P_{\ell-1} B_{\ell-2} \in \mathbb{R}^{N_{\ell-1} \times N}$  expressed in a recursive manner and  $B_0 = A_0$ .

With this definitions in place, we can state the main theorem:

**Theorem 3.2** (Main result). *Matrices  $L_c$  and  $L$  are  $(\mathcal{R}, \epsilon)$ -similar whenever*

$$\epsilon = \sum_{\ell=1}^c \epsilon_\ell \prod_{q=1}^{\ell-1} (1 + \epsilon_q) \leq 1,$$

where  $\epsilon_\ell = \|\Pi_\ell^\perp A_{\ell-1}\|_{L_{\ell-1}}$  for each level  $\ell$ .

This result is fairly general as it holds for any PSD matrix  $L$ , number of levels  $c$ , and matrices  $P_1, P_2, \dots, P_c$ .

### 3.2 Spectrum approximation guarantees

One of the key benefits of restricted similarity is that it implies a relation between the spectra of matrices  $L$  and  $L_c$  that goes beyond interlacing (see Theorem 2.3).

To this effect, consider the smallest  $k$  eigenvalues and respective eigenvectors and define the following matrices:

$$U_k \in \mathbb{R}^{N \times k} = [u_1, u_2, \dots, u_k] \quad \text{and} \quad \Lambda_k = \text{diag}(\lambda_1, \lambda_2, \dots, \lambda_k)$$

Further, let  $\mathcal{U}_k$  be the column-space of  $U_k$ . As we will show next, ensuring that  $\epsilon$  in Theorem 3.2 is small when  $\mathcal{R} = \mathcal{U}_k$  suffices to guarantee that the first  $k$  eigenvalues and eigenvectors of  $L$  and  $L_c$  are aligned.

Before stating these results formally, let us note that Theorem 3.2 simplifies when  $\mathcal{R}$  is an eigenspace of  $L$ . We demonstrate this for the choice of  $\mathcal{U}_k$ , though an identical argument can be easily derived for any eigenspace: by the unitary invariance of the spectral norm, Theorem 3.2 also holds for  $B_0 U$  where  $U$  is the full eigenvector matrix. Eliminating zero rows, we have that  $B_0 = U_k \Lambda_k^{-1/2} \in \mathbb{R}^{N \times k}$ . This is computationally attractive because now at each level one needs to take the pseudo-inverse-square-root of a much smaller matrix  $B_{\ell-1}^\top L_{\ell-1} B_{\ell-1} \in \mathbb{R}^{k \times k}$ .

We now present our first spectrum approximation result next:

**Theorem 3.3** (Eigenvalue approximation). *If  $L_c$  and  $L$  are  $(\mathcal{U}_k, \epsilon_k)$ -similar, then*

$$\lambda_k \leq \tilde{\lambda}_k \leq \frac{(1 + \epsilon_k)^2}{1 - \|\Pi^\perp U_k\|_2^2} \lambda_k.$$

Term  $\|\Pi^\perp U_k\|_2^2$  is only indirectly dependent of  $L$  and measures the worse-case error when we attempt to approximate vectors  $x = U_k a$  by  $\Pi x$  for all  $a \in \mathbb{R}^k$ .

Noticing that  $\epsilon_k \leq \epsilon_{k'}$  and  $\|\Pi^\perp U_k\|_2 < \|\Pi^\perp U_{k'}\|_2$  whenever  $k < k'$ , we deduce that the bound is stronger for smaller eigenvalues. Observe also that the proposed upper bound depends on  $\lambda_k$  instead of  $\lambda_{k+N-n}$  and thus can be significantly tighter than the one given by Theorem 2.3.

We also analyze the angle between principal eigenspaces of  $L$  and  $L_c$ . We follow [25] and split the (lifted) eigendecompositions of  $L = U \Lambda U^\top$  and  $L_c = \tilde{U} \tilde{\Lambda} \tilde{U}^\top$  as

$$L = (U_k, U_{k^\perp}) \begin{pmatrix} \Lambda_k & \\ & \Lambda_{k^\perp} \end{pmatrix} \begin{pmatrix} U_k^\top \\ U_{k^\perp}^\top \end{pmatrix} \quad P^\top L_c P = (P^\top \tilde{U}_k, P^\top \tilde{U}_{k^\perp}) \begin{pmatrix} \tilde{\Lambda}_k & \\ & \tilde{\Lambda}_{k^\perp} \end{pmatrix} \begin{pmatrix} \tilde{U}_k^\top P \\ \tilde{U}_{k^\perp}^\top P \end{pmatrix},$$

where  $\tilde{\Lambda}_k$  and  $\tilde{U}_k$  are defined analogously to  $\Lambda_k$  and  $U_k$ . Davis and Kahan [8] defined the *canonical angles* between the spaces spanned by  $U_k$  and  $P^\top \tilde{U}_k$  as the singular values of the matrix

$$\Theta(U_k, P^\top \tilde{U}_k) \triangleq \arccos(U_k^\top P^\top \tilde{U}_k \tilde{U}_k^\top P U_k)^{-1/2},$$

see also [35]. The smaller the sinus of the canonical angles are the closer the two subspaces lie.

The following theorem characterizes the miss-alignment of the eigenspaces spanned by  $U_k$  and lifted  $\tilde{U}_k$ .

**Theorem 3.4** (Eigenspace approximation). *If  $L_c$  and  $L$  are  $(\mathcal{U}_k, \epsilon_k)$ -similar then*

$$\|\sin \Theta(U_k, P^\top \tilde{U}_k)\|_F^2 \leq \sum_{i=1}^k \frac{\epsilon_k(2 + \epsilon_k) \lambda_i + \lambda_k \|\Pi^\perp u_i\|_2^2}{\tilde{\lambda}_{k+1} - \lambda_k}.$$

As described in the proof, the theorem can be improved slightly by substituting  $\epsilon_k$  in the  $i$ -th term of the sum with the minimum  $\epsilon_i \leq \epsilon_k$  such that  $L_c$  and  $L$  are  $(\mathcal{U}_i, \epsilon_i)$ -similar. Due to the interlacing theorem, if desired we can also substitute  $\tilde{\lambda}_{k+1}$  in the denominator by  $\lambda_{k+1}$  without any problem.

### 3.3 Implications for Laplacian matrices

For consistent coarsening the spectrum approximation results presented previously imply certain structural similarities between the cut-structure of  $G_c$  and  $G$ . Intuitively, if the coarsening is done well and  $G_c$  contains a good cut, then so will  $G$ .

We formalize this statement for the case of graph bisection: For any subset  $S$  of  $\mathcal{V}$ , we use  $\partial S := \{e_{ij} \in E : v_i \in S, v_j \in \mathcal{V} \setminus S\}$  to denote the set of edges going from a vertex in  $S$  to a vertex not in  $S$ . The *isoperimetric constant* of graph  $G$  is

$$i(G) = \min_{0 < |S| \leq \frac{N}{2}} \frac{e(S, \bar{S})}{|S|}, \quad (4)$$

where  $e(S, \bar{S}) = \sum_{e_{ij} \in \partial S} w_{ij}$ . The smaller  $i(G)$  is, the easier it is to cut the graph in two.

As it turns out, the isoperimetric constants  $i(G)$  and  $i(G_c)$  are closely related:

**Corollary 3.5.** *If  $L_c$  and  $L$  are  $(\mathcal{U}_2, \epsilon)$ -similar combinatorial Laplacian matrices then*

$$i(G) \leq i(G_c) \leq 2 \frac{(1 + \epsilon)}{\|\Pi u_2\|_2} \sqrt{d_{\max}(G_c) i(G)},$$

where  $d_{\max}(G_c)$  is the maximum weighted degree of  $G_c$ .

This is a non-constructive result: it does not reveal how to find the optimal bisection, but provides conditions such that the latter is of similar quality in the two graphs. We remark that a slightly more involved argument (involving the normalized Laplacian) can also be used to show that coarsening with good restricted similarity preserves conductance.

Based on Theorem 3.4, it is also possible to derive approximation results about the solution quality of two unsupervised learning algorithms that utilize  $U_k$  in order to cluster and draw  $G$ : spectral clustering and Laplacian eigenmaps. We do not include the derivation here since it is almost identical to that found in [27] (see also [1, 28]).

## 4 Consistent coarsening by local variation

This section proposes algorithms for consistent graph coarsening. That is, we suppose that  $L$  is a combinatorial graph Laplacian and that the coarsening matrices are designed according to the guidelines given in Section 2.4.

As we saw in Section 2.3, graph coarsening boils down to deciding for each level  $\ell$  a partitioning of  $\mathcal{V}_{\ell-1}$  into  $N_\ell$  contraction sets  $\mathcal{P}_\ell = \{\mathcal{V}_{\ell-1}^{(1)}, \dots, \mathcal{V}_{\ell-1}^{(N_\ell)}\}$ . Every coarse vertex  $v'_r \in \mathcal{V}_\ell$  is then formed by contracting the vertices in  $\mathcal{V}_{\ell-1}^{(r)}$ . In addition, according to Theorem 3.2, the resulting graph Laplacian  $L_c$  will be similar to  $L$  if, for each level, the following *variation cost* is as small as possible:

$$\epsilon_\ell = \|\Pi_\ell^\perp A_{\ell-1}\|_{L_{\ell-1}}, \quad (5)$$

with  $A_{\ell-1}$  being a matrix that depends on the subspace of interest as well as the decisions taken at levels 1 to  $\ell - 1$ . Finally, to avoid compounding errors, we aim to achieve the largest possible reduction as early as possible.

The main difficulty with minimizing  $\epsilon_\ell$  is that it does not depend only on some property of contraction sets independently, but also on their interactions. This is a particularity of coarsening

that distinguishes it from edge-sparsification and emerges due to the interaction of the projection matrix and the Laplacian-induced semi-norm<sup>1</sup>.

Nonetheless, as we show next, it is possible to ignore without significant loss the interactions between contraction sets and consider each *local variation cost* (i.e., the cost of contracting solely the vertices in  $\mathcal{V}^{(r)}$ ) independently. Having achieved this, Section 4.2 considers ways of efficiently identifying families of disjoint sets with small local variation cost.

## 4.1 The decoupling argument

Suppose that  $\Pi_{\mathcal{C}}^\perp$  is the (complement) projection matrix obtained by contracting solely the vertices in set  $\mathcal{C}$ , while leaving all other vertices in  $\mathcal{V}_{\ell-1}$  untouched:

$$[\Pi_{\mathcal{C}}^\perp x](i) = \begin{cases} x(i) - \sum_{v_j \in \mathcal{C}} \frac{x(j)}{|\mathcal{C}|} & \text{if } v_i \in \mathcal{C} \\ 0 & \text{otherwise.} \end{cases}$$

(Here, for convenience, the level index is suppressed.)

Furthermore, let  $L_{\mathcal{C}}$  be the  $N_{\ell-1} \times N_{\ell-1}$  combinatorial Laplacian whose weight matrix is

$$[W_{\mathcal{C}}](i, j) = \begin{cases} W_{\ell-1}(i, j) & \text{if } v_i, v_j \in \mathcal{C} \\ 2W_{\ell-1}(i, j) & \text{if } v_i \in \mathcal{C} \text{ and } v_j \notin \mathcal{C} \\ 0 & \text{otherwise.} \end{cases} \quad (6)$$

That is,  $W_{\mathcal{C}}$  is zero everywhere other than at the edges touching at least one vertex in  $\mathcal{C}$ . The following lemma shows us how to decouple the contribution of each contraction set to the variation cost.

**Theorem 4.1.** *The variation cost  $\epsilon_\ell$  is smaller than  $\sqrt{\sum_{\mathcal{C} \in \mathcal{P}} \|\Pi_{\mathcal{C}}^\perp A_{\ell-1}\|_{L_{\mathcal{C}}}^2}$ .*

The decoupling argument therefore entails bounding the, difficult to optimize, variation cost as a function of locally computable and independent costs  $\|\Pi_{\mathcal{C}}^\perp A_{\ell-1}\|_{L_{\mathcal{C}}}^2$ . The obtained expression is a relaxation, as it assumes that the interaction between contraction sets will be the worst possible. It might be interesting to notice that the quality of the relaxation depends on the weight of the cut between contraction sets. Taking the limit, the inequality converges to an equality as the weight of the cut shrinks. Also of note, the bound becomes tighter the larger the dimensionality reduction requested (since  $n_\ell = |\mathcal{P}|$ , the smaller  $n_\ell$  is, the fewer inequalities are involved in the derivation).

## 4.2 Contraction families and local variation coarsening

Starting from a *contraction family*  $\mathcal{F}_\ell = \{\mathcal{C}_1, \mathcal{C}_2, \mathcal{C}_3, \dots\}$ , that is, an appropriately sized family of candidate contraction sets, our strategy will be to search for a small partitioning  $\mathcal{P}_\ell$  of  $\mathcal{V}_{\ell-1}$  with minimal variation cost  $\epsilon_\ell$ .

As a thought experiment, suppose that set  $\mathcal{C}$  is chosen to be part of  $\mathcal{P}_\ell$ . From the decoupling argument, its contribution to  $\epsilon_\ell^2$  will be at most  $\|\Pi_{\mathcal{C}}^\perp A_{\ell-1}\|_{L_{\mathcal{C}}}^2$ , independently of how the other candidate sets are chosen. Moreover, the selection will yield a reduction of  $N_{\ell-1}$  by  $|\mathcal{C}| - 1$  vertices.

---

<sup>1</sup>Even though the projection matrix  $\Pi_{\mathcal{C}}^\perp$  is block diagonal, the presence of the gradient matrix  $S_{\ell-1}$  introduces a dependency between adjacent contraction sets.

Thus, we look for the non-singleton candidate sets  $\mathcal{C}$  with cost

$$\text{cost}_\ell(\mathcal{C}) \triangleq \frac{\|\Pi_{\mathcal{C}}^\perp A_{\ell-1}\|_{L_{\mathcal{C}}}^2}{|\mathcal{C}| - 1} \quad (7)$$

that is as small as possible. We refer to (7) as *local variation cost* because it captures the maximal variation of all signals from an appropriate subspace (defined by  $A_{\ell-1}$ ) with support on  $\mathcal{C}$ . On the other hand, since any permissible family  $\mathcal{P}_\ell$  of contraction sets should be a partitioning of  $\mathcal{V}_{\ell-1}$ , choosing  $\mathcal{C}$  precludes us from selecting any  $\mathcal{C}'$  with which it intersects.

Based on this intuition, Algorithm 1 sequentially examines candidate sets from  $\mathcal{F}_\ell$ , starting from those with minimal cost. To decide whether a candidate set  $\mathcal{C}$  will be added to  $\mathcal{P}_\ell$  the algorithm asserts that all vertices in  $\mathcal{C}$  are unmarked—essentially enforcing that all contraction sets are disjoint. Accordingly, as soon as  $\mathcal{C}$  is added to  $\mathcal{P}_\ell$ , all vertices that are in  $\mathcal{C}$  become marked. Candidate sets with marked vertices are pruned ( $\mathcal{C}' \leftarrow \mathcal{C} \setminus \text{marked}$ ) and their cost is recomputed. The algorithm terminates if there are no more candidates in  $\mathcal{F}_\ell$  or if the target reduction  $r$  is achieved. Even though this remains implicit in the discussion, if at termination  $\mathcal{P}_\ell$  does not cover every vertex of  $\mathcal{V}_{\ell-1}$ , then we compliment it with singleton sets, featuring one vertex each (and zero cost).

---

**Algorithm 1** Coarsening by local variation

---

```

1: input: A family of candidate sets  $\mathcal{F}_\ell = \{\mathcal{C}_1, \mathcal{C}_2, \mathcal{C}_3, \dots\}$  and a target reduction  $r$ .
2:  $N_\ell \leftarrow N_{\ell-1}$ , marked  $\leftarrow \emptyset$ 
3: Sort  $\mathcal{F}_\ell$  in terms of increasing  $\text{cost}_\ell(\mathcal{C})$ .
4: while  $|\mathcal{F}_\ell| > 0$  and  $r > 1 - N_\ell/N_{\ell-1}$  do
5:   Pop the candidate set  $\mathcal{C}$  of minimal cost from  $\mathcal{F}_\ell$ .
6:   if all vertices of  $\mathcal{C}$  are not marked then
7:     marked  $\leftarrow \text{marked} \cup \mathcal{C}$ ,  $\mathcal{P}_\ell \leftarrow \mathcal{P}_\ell \cup \mathcal{C}$ ,  $N_\ell \leftarrow N_\ell - |\mathcal{C}| + 1$ 
8:   else
9:      $\mathcal{C}' \leftarrow \mathcal{C} \setminus \text{marked}$ 
10:    if  $|\mathcal{C}'| > 1$  then
11:      Compute  $\text{cost}_\ell(\mathcal{C}')$  and insert  $\mathcal{C}'$  into  $\mathcal{F}_\ell$  while keeping the latter sorted.
12: return  $\mathcal{P}_\ell$ 

```

---

Undeniably, Algorithm 1 is only one of the possible ways to select a partitioning of small variation cost. However, this algorithm stands out from other algorithms we experimented with, as it is very efficient when the subspace of interest is an eigenspace (e.g.,  $V = U_k$ ),  $k$  is small, and the families  $\mathcal{F}_\ell$  have been selected appropriately. To see this, denote by  $\Phi = \max_\ell \sum_{\mathcal{C} \in \mathcal{F}_\ell} |\mathcal{C}|$  the maximum number of vertices in all candidate sets and by  $\delta = \max_{\ell, \mathcal{C} \in \mathcal{F}_\ell} |\mathcal{C}|$  the cardinality of the maximum candidate set—we refer to these measures as *family size* and *width*, respectively. Choosing  $\mathcal{R} = \mathcal{U}_k$ , the computational complexity of Algorithm 1 is  $O(ckM + k^2N + ck^3 + c\Phi(\min\{k^2\delta + k\delta^2, k\delta^2 + \delta^3\} + \log |\mathcal{F}_\ell|))$ , which is linear on the number of levels, edges, vertices, and  $\Phi$  (see Appendix B for details).

If computational complexity is of little (or no) concern, one may consider the following two more sophisticated algorithms: *The optimal algorithm*. Given a candidate family, the algorithm that optimally minimizes the sum of local variation costs constructs a graph with one vertex for each subset of a candidate set and adds an edge between every two vertices whose respective sets have a non-empty intersection. It then selects  $\mathcal{P}_\ell$  as the maximum independent set of minimal weight (the weight of each vertex is a local variation cost w.r.t a set). Unfortunately, the minimum-weight independent set problem is NP-hard. Nevertheless, for the specific case where candidate sets

correspond to edges, the problem simplifies to a minimum-weight matching problem, which can be computed in  $O(N_{\ell-1}^3)$  time. *The quadratic variant.* A second possibility is to proceed as with Algorithm 1, but to prune each  $\mathcal{C}' \in \mathcal{F}_\ell$  after a set  $\mathcal{C}$  is added to  $\mathcal{P}_\ell$ . Our experiments indicated that this additional step improves slightly the coarsening quality, but we do not recommend it for large graphs as it introduces a quadratic dependency of the complexity on  $N$ .

**Contraction families.** To keep Algorithm 1 efficient, we recommend using families of linear size and poly-logarithmic width w.r.t.  $M$ . We consider two possibilities:

*Edge-based.* Here  $\mathcal{F}_\ell$  contains one candidate set for each edge of  $G_{\ell-1}$ . This is a natural choice for coarsening—indeed, most coarsening algorithms in the literature use some form of edge contraction. It is straightforward to see that in this case  $\Phi = 2M$  and  $\delta = 2$ , meaning that the expression of the computational complexity simplifies to  $O(cM(k + \log M) + ck^3 + k^2N)$ . The drawback of contracting edges is that at each level the graph size can only reduce by at most a factor of 2, meaning that a large number of levels is necessary to achieve significant reduction<sup>2</sup>.

*Neighborhood-based.* A more attractive choice is to construct one candidate set for the neighborhood of each vertex, including the vertex itself. Denoting by  $\Delta$  the largest combinatorial degree and since  $\Phi = 2M$ , the complexity here is bounded by  $O(cM(k + \log N + \min\{k^2\Delta + k\Delta^2, k\Delta^2 + \Delta^3\}) + ck^3 + k^2N)$ . Our experiments show that the neighborhood-based construction generally achieves better reduction, while being marginally slower than edge-based families.

## 5 Numerical results

We performed our evaluation primarily based on four representative graphs, each exhibiting different structural characteristics:

- *Yeast.* Protein-to-protein interaction network in budding yeast, analyzed by Jeong et al. [19]. The network has  $N = 1458$  vertices,  $M = 1948$  edges, diameter of 19, and degree between 1 and 56.
- *Airfoil.* Finite-element graph obtained by airflow simulation [29], consisting of  $N = 4000$  vertices,  $M = 11490$  edges, diameter of 65, and degree between 1 and 9.
- *Minnesota.* Road network with  $N = 2642$  vertices,  $M = 3304$  edges, diameter of 99, and degree between 1 and 5 [15].
- *Bunny.* Point cloud consisting of  $N = 2503$  vertices,  $M = 65490$  edges, diameter of 15, and degree between 13 and 97 [36]. The point cloud has been sub-sampled from its original size.

We compare to the following methods for multilevel graph coarsening:

- *Heavy edge matching.* At each level of the scheme, the contraction family is obtained by computing a maximum-weight matching with the weight of each contraction set (i.e.,  $(v_i, v_j)$ ) calculated as  $w_{ij} / \max\{d_i, d_j\}$ . In this manner, heavier edges connecting vertices that are well separated from the rest of the graph are contracted first. Heavy edge matching was first introduced in the algebraic multigrid literature and, perhaps due to its simplicity, it has been repeatedly used for partitioning [20, 10] and drawing [38, 18] graphs, as well as more recently in graph convolutional neural networks [9].

---

<sup>2</sup>In practice, depending on the topology of the graph in question, the per-level reduction ratio  $r_\ell$  is usually between 0.35 and 0.45.

- *Algebraic distance.* This method differs from heavy edge matching in that the weight of each contraction set is calculated as  $(\sum_{q=1}^Q (x_q(i) - x_q(j))^2)^{1/2}$ , where  $x_k$  is an  $N$ -dimensional test vector computed by successive sweeps of Jacobi relaxation. The complete method is described by Ron et al. [30], see also [5]. As recommended by the authors, we perform 20 relaxation sweeps. We set the number of test vectors  $Q$  to equal the dimension  $k$  of the space we aim to approximate (a simple rank argument shows that  $Q \geq k$  for the test vectors to span the space).
- *Affinity.* This is a vertex proximity heuristic in the spirit of the algebraic distance that was proposed by Livne and Brandt [26] in the context of their work on the lean algebraic multigrid. As per author suggestion, the  $Q = k$  test vectors are here computed by a single sweep of a Gauss–Seidel iteration.
- *Kron reduction.* At each level, the graph size is reduced by selecting a set of vertices of size  $N/2$  (corresponding to the positive entries of the last eigenvector of  $L$ ) and applying Kron reduction. The method, which was proposed by [32], is not strictly a coarsening method as it completely rewrites the vertices of the reduced graph, resulting in significantly denser graphs<sup>3</sup>. Unfortunately, the rewiring step entails finding the Schur complement of a large Laplacian submatrix and thus generally exhibits  $O(N^3)$  complexity, rendering it prohibitive for graphs of more than a few thousand vertices. Despite these drawbacks, the method is quite popular because of its elegant theoretical guarantees [11].

Depending on how the edge matching is constructed, different variants of edge contraction methods can be implemented. At the two extremes of the complexity spectrum one finds the maximum matching of minimum weight at a complexity of  $O(N^3)$  [12] or greedily constructs a matching by visiting vertices in a random order and inducing  $O(M)$  overhead [10].

For consistency, we implement all edge-based methods by combining Algorithm 1 with an edge-based family and substituting the local variation cost with the (negative) method-specific edge weight. This generally yields matchings of better quality (heavier weight) than visiting vertices in a predefined order, at the expense of the marginally larger  $O(M \log M)$  complexity necessary for sorting the edge weights. Our choice is also motivated by the observation that the computational bottleneck of (sophisticated) edge contraction methods lies in the edge weight computation.

## 5.1 Restricted similarity

Our first experiment tests how well  $L_c$  approximates the action of  $L$  with respect to the subspace  $U_k$  of smallest variation. In other words, for each method we plot the smallest  $\epsilon$  such that the following equation holds:

$$(1 - \epsilon) \|x\|_L \leq \|x_c\|_{L_c} \leq (1 + \epsilon) \|x\|_L, \quad (8)$$

for every vector  $x \in U_k$ .

The results are summarized in Figure 2 for two representative subspaces of size  $k = 10$  and  $k = 40$ . With the exception of the Kron reduction that was repeated 10 times, all methods are deterministic and thus were run only once.

Overall, it can be seen that local variation methods outperform other coarsening methods in almost every problem instance. The accuracy gap is particularly prominent for large reductions,

---

<sup>3</sup>As suggested by the authors, the sparsity of reduced graphs can be controlled by spectral sparsification. We did not include the sparsification step in our numerical experiments since it often resulted in increased errors.

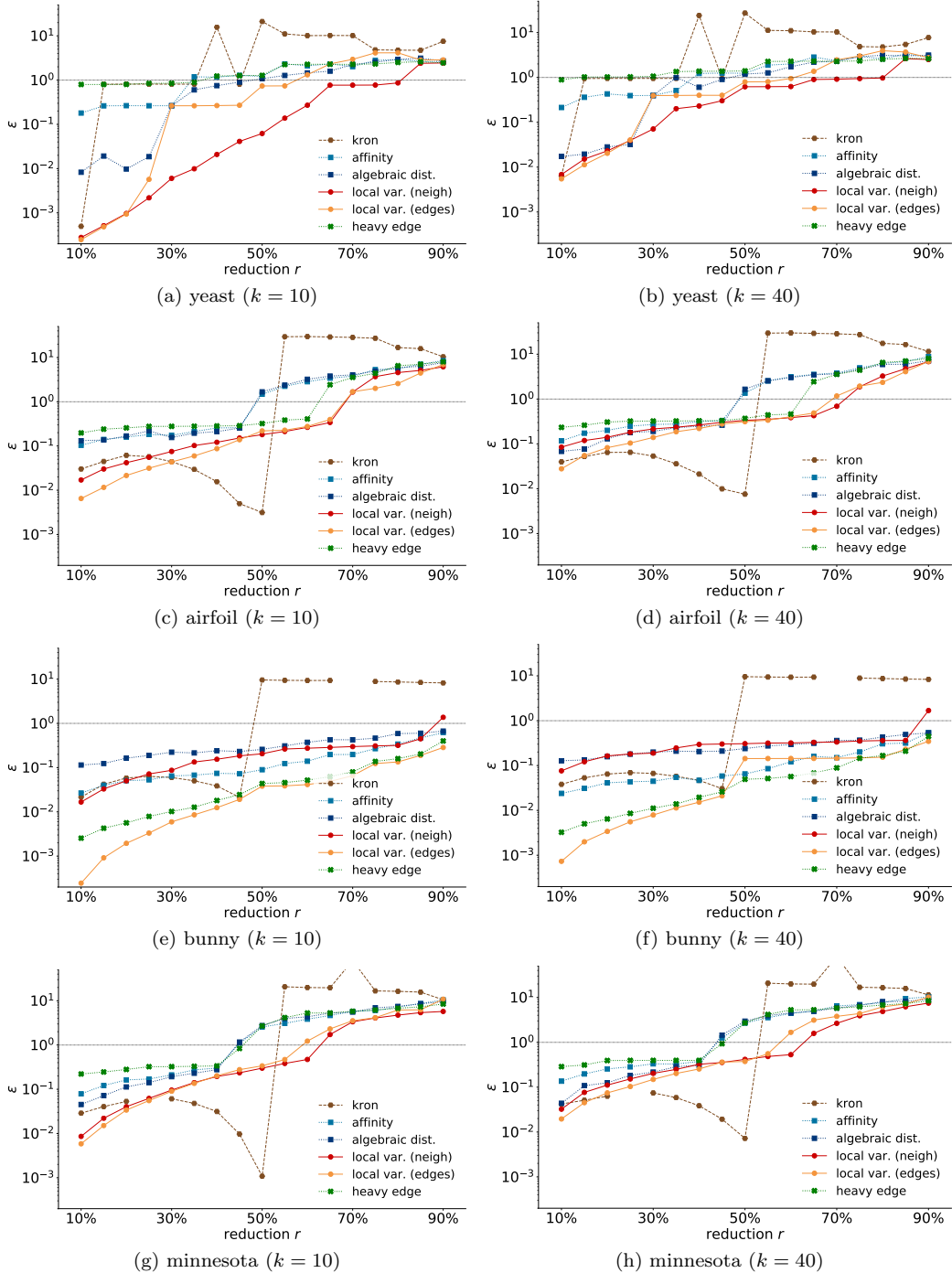


Figure 2: Quality of approximation comparison for four representative graphs (rows) and two subspace sizes (columns).

where multiple levels are employed. Neighborhood-based contraction yields the best result overall, mainly because it achieves the same reduction in fewer levels. Interestingly, local variation (and

coarsening) methods in many cases also outperform Kron reduction, even though the latter is more demanding computationally.

We elaborate further on four points stemming from the results:

*In most instances, a reduction of up to 70% is feasible while maintaining a decent approximation.* The attained approximation clearly is a function of the graph in question and  $k$ . Nevertheless, in almost all experiments, the best coarsening method could reduce the graph size by at least 70% while also ensuring that  $\epsilon < 1$  (horizontal black line). This is an encouraging sign, illustrating that significant dimensionality reduction is often possible, without sacrificing too much the solution quality.

*Following intuition, it is generally harder to approximate subspaces of larger dimension  $k$ , but not excessively so.* Increasing  $k$  from 10 to 40 in most cases increases  $\epsilon$  only slightly. The only case where the approximation becomes profoundly better with small subspaces is with small reduction ratios  $r$ . For instance, coarsening the yeast graph results in an impressive approximation for all  $r < 30\%$  when  $k = 10$ , whereas  $\epsilon$  increases almost by an order of magnitude when  $k$  becomes 40.

*Kron reduction is an effective way to half the graph size but can result in poor approximation otherwise.* If one is willing to sacrifice in terms of efficiency, Kron reduction effectively reduces the size of the graph by a factor of two (with the exception of the yeast graph). What might be startling is that the method behaves poorly for different reduction ratios. Three main factors cause this deterioration of performance. First, the sampling set is constructed based on the polarity of  $u_N$  and has cardinality close to  $N/2$  [32]. Therefore, if in any level we try to reduce the graph size by less than half, the last eigenvector heuristic cannot be used exactly. Second, numerical instability issues sometimes manifest when  $r$  exceeds 50%. Though we attempted to improve the original implementation featured in the PyGSP toolbox, some problem instances could not be solved successfully (hence the missing markers). The third reason is described next.

*Coarse levels should aim to approximate the original graph and not the proceeding levels.* The conventional approach in multilevel schemes is to aim at each level to approximate as closely as possible the graph of the previous level. This can lead to sudden increase of error at consecutive levels (e.g. notice the minnesota error as  $r$  approaches 50%) as decisions early in the scheme can have a large impact later on. On the other hand, following Theorem 3.2 local variation methods modify the cost function minimized at each level, resulting in smoother transitions between levels and tighter approximations at large  $r$ .

## 5.2 Spectrum approximation

The second part of our experiments examines the coarsening through the lens of spectral graph theory. Our premise is that, since the spectrum of the Laplacian distills information about the graph structure, we can interpret the spectral distance as a proxy for the structural similarity of the two graphs. This is by no means a new idea—the Laplacian spectrum is a common ingredient in accessing graph similarity [41].

Tables 1 and 2 report the mean relative eigenvalue error defined as  $\frac{1}{k} \sum_{i=1}^k \frac{|\tilde{\lambda}_i - \lambda_i|}{\lambda_i}$  for two representative  $k$ , respectively 10 and 40. The results for  $k = 80$  were consistent with those presented here, and are not reported here for reasons of brevity.

As expected, the reduction ratio plays a major role in the closeness of Laplacian spectra. Indeed, for most cases the eigenvalue error jumps by almost an order of magnitude whenever  $r$  increases by 20%. Yet, in most cases we can achieve acceptable errors even when the coarse graph is as small as one third of the size of the original graph (corresponding to  $r = 70\%$ ).

	$r$	heavy edge	local var. (edges)	local var. (neigh.)	algebraic distance	affinity	Kron reduction
yeast	30%	0.343	0.123	<b>0.003</b>	0.145	0.177	0.054
	50%	0.921	0.459	<b>0.034</b>	0.605	1.020	1.321
	70%	3.390	3.495	<b>0.406</b>	3.504	3.732	1.865
airfoil	30%	0.277	<b>0.036</b>	0.065	0.213	0.245	0.352
	50%	0.516	0.201	<b>0.197</b>	1.268	1.375	0.912
	70%	4.744	1.045	<b>0.928</b>	5.544	5.775	1.984
bunny	30%	0.019	<b>0.006</b>	0.061	0.277	0.068	0.335
	50%	0.064	<b>0.046</b>	0.190	0.435	0.135	0.801
	70%	0.126	<b>0.081</b>	0.323	0.692	0.295	1.812
minnesota	30%	0.332	0.088	<b>0.078</b>	0.232	0.280	0.318
	50%	2.018	0.432	<b>0.310</b>	2.398	2.426	0.882
	70%	9.299	4.579	<b>1.866</b>	9.938	9.177	1.951

Table 1: Mean relative error for the first  $k = 10$  eigenvalues, for different graphs, reduction ratios, and coarsening methods.

	$r$	heavy edge	local var. (edges)	local var. (neigh.)	algebraic distance	affinity	Kron reduction
yeast	30%	0.328	0.113	<b>0.023</b>	0.094	0.195	0.120
	50%	0.879	0.430	<b>0.130</b>	0.517	0.769	1.196
	70%	2.498	2.182	<b>0.451</b>	2.560	2.229	1.946
airfoil	30%	0.277	<b>0.095</b>	0.181	0.189	0.267	0.368
	50%	0.549	<b>0.325</b>	0.349	0.698	0.862	0.960
	70%	2.268	0.872	<b>0.839</b>	2.373	2.531	2.078
bunny	30%	0.023	<b>0.008</b>	0.085	0.205	0.052	0.294
	50%	0.066	<b>0.058</b>	0.181	0.346	0.089	0.660
	70%	0.128	<b>0.098</b>	0.299	0.509	0.202	1.192
minnesota	30%	0.353	0.118	<b>0.115</b>	0.209	0.306	0.337
	50%	1.259	0.468	<b>0.383</b>	1.342	1.264	0.933
	70%	4.162	2.111	<b>1.612</b>	4.145	4.185	2.090

Table 2: Mean relative error for the first  $k = 40$  eigenvalues, for different graphs, reduction ratios, and coarsening methods.

It might also be interesting to observe that there is a general agreement between the trends reported here and those described in the matrix approximation experiment. In particular, if we sort the tested methods from best to worse, we will obtain an ordering that is consistent across the two experiments, with local variation methods giving the best approximation by a significant margin. A case in point: for the maximum ratio, the best local variation method is on average  $3.9\times$  better than the leading state-of-the-art coarsening method. The gain is  $2.6\times$  if we also include Kron reduction in the comparison.

Overall, we can see deduce from these results that local variation methods coarsen a graph in a manner that preserves its spectrum. This is in accordance with our theoretical results. As we saw in Theorem 3.3, if  $L$  and  $L_c$  act similar w.r.t. all vectors in  $U_k$ , then their eigenvalues cannot be far apart. Therefore, by aiming for increased similarity, local variation methods implicitly also guarantee spectrum approximation.

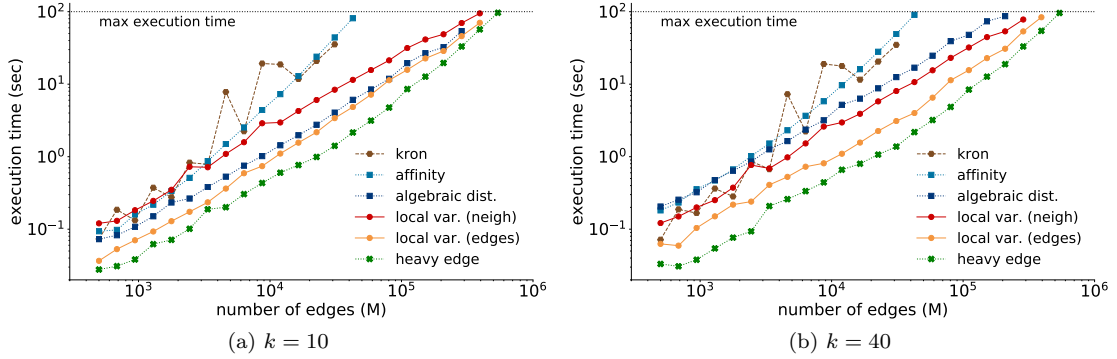


Figure 3: Execution time as a function of the number of edges of the graph.

### 5.3 Efficiency

Our last experiment tests computational efficiency. We adopt a simple approach and aim to coarsen a 10-regular graph of increasing size. We measure the execution time of the six different methods for graph reduction and report the mean over 10 iterations.

The results are displayed in Figures 3a and 3b for subspaces of size 10 and 40, respectively. As with most such comparisons, the actual numbers are only indicative and depend on the programming language utilized (Python), processing paradigm (no parallelism was employed), and hardware architecture (2.2GHz CPU)<sup>4</sup>.

Focusing on the trends, with the exception of Kron reduction and affinity, most methods scale quasi-linearly with the number of edges. Interestingly, local variation methods are quite competitive and do not sacrifice much as compared to the straightforward heavy edge matching. We can also observe that constructing  $\mathcal{F}_{\ell-1}$  based on neighborhoods results in slightly slower computation than with the edge-based method construction, because in the latter case the local variation cost can be computed much more efficiently.

## References

- [1] Christos Boutsidis, Anastasios Zouzias, Michael W Mahoney, and Petros Drineas. Randomized dimensionality reduction for k-means clustering. *IEEE Transactions on Information Theory*, 61(2):1045–1062, 2015.
- [2] M. M. Bronstein, J. Bruna, Y. LeCun, A. Szlam, and P. Vandergheynst. Geometric deep learning: Going beyond euclidean data. *IEEE Signal Processing Magazine*, 34(4):18–42, July 2017.
- [3] Joan Bruna, Wojciech Zaremba, Arthur Szlam, and Yann Lecun. Spectral networks and locally connected networks on graphs. In *International Conference on Learning Representations (ICLR2014), CBLS, April 2014*, 2014.
- [4] Guantao Chen, George Davis, Frank Hall, Zhongshan Li, Kinnari Patel, and Michael Stewart. An interlacing result on normalized laplacians. *SIAM Journal on Discrete Mathematics*, 18(2):353–361, 2004.

<sup>4</sup>We expect that a significant speedup can be achieved by compiling the code to native machine instructions as well as by parallelizing the local variation cost computation.

- [5] Jie Chen and Ilya Safro. Algebraic distance on graphs. *SIAM Journal on Scientific Computing*, 33(6):3468–3490, 2011.
- [6] Fan RK Chung. *Spectral graph theory*. Number 92. American Mathematical Soc., 1997.
- [7] Charles Colley, Junyuan Lin, Xiaozhe Hu, and Shuchin Aeron. Algebraic multigrid for least squares problems on graphs with applications to hodgerank. In *Parallel and Distributed Processing Symposium Workshops (IPDPSW), 2017 IEEE International*, pages 627–636. IEEE, 2017.
- [8] Chandler Davis and William Morton Kahan. The rotation of eigenvectors by a perturbation. iii. *SIAM Journal on Numerical Analysis*, 7(1):1–46, 1970.
- [9] Michaël Defferrard, Xavier Bresson, and Pierre Vandergheynst. Convolutional neural networks on graphs with fast localized spectral filtering. In *Advances in Neural Information Processing Systems*, pages 3844–3852, 2016.
- [10] Inderjit S Dhillon, Yuqiang Guan, and Brian Kulis. Weighted graph cuts without eigenvectors a multilevel approach. *IEEE transactions on pattern analysis and machine intelligence*, 29(11), 2007.
- [11] Florian Dörfler and Francesco Bullo. Kron reduction of graphs with applications to electrical networks. *IEEE Trans. on Circuits and Systems*, 60(1):150–163, 2013.
- [12] Zvi Galil. Efficient algorithms for finding maximum matching in graphs. *ACM Computing Surveys (CSUR)*, 18(1):23–38, 1986.
- [13] Shivam Gandhi. Improvement of the cascadic multigrid algorithm with a gauss seidel smoother to efficiently compute the fiedler vector of a graph laplacian. *arXiv preprint arXiv:1602.04386*, 2016.
- [14] Matan Gavish, Boaz Nadler, and Ronald R Coifman. Multiscale wavelets on trees, graphs and high dimensional data: Theory and applications to semi supervised learning. In *ICML*, pages 367–374, 2010.
- [15] David Gleich. Matlabbgl. a matlab graph library. *Institute for Computational and Mathematical Engineering, Stanford University*, 2008.
- [16] Bruce Hendrickson and Robert W Leland. A multi-level algorithm for partitioning graphs. *SC*, 95(28):1–14, 1995.
- [17] Anil N Hirani, Kaushik Kalyanaraman, and Seth Watts. Graph laplacians and least squares on graphs. In *Parallel and Distributed Processing Symposium Workshop (IPDPSW), 2015 IEEE International*, pages 812–821. IEEE, 2015.
- [18] Yifan Hu. Efficient, high-quality force-directed graph drawing. *Mathematica Journal*, 10(1):37–71, 2005.
- [19] H. Jeong, S.P. Mason, A.L. Barabasi, and Z.N. Oltvai. Lethality and centrality in protein networks. *arXiv preprint cond-mat/0105306*, 2001.
- [20] George Karypis and Vipin Kumar. A fast and high quality multilevel scheme for partitioning irregular graphs. *SIAM Journal on scientific Computing*, 20(1):359–392, 1998.
- [21] David Harel Yehuda Koren. A fast multi-scale method for drawing large graphs. *Journal of graph algorithms and applications*, 6(3):179–202, 2002.

- [22] Ioannis Koutis, Gary L Miller, and David Tolliver. Combinatorial preconditioners and multilevel solvers for problems in computer vision and image processing. *Computer Vision and Image Understanding*, 115(12):1638–1646, 2011.
- [23] Dan Kushnir, Meirav Galun, and Achi Brandt. Fast multiscale clustering and manifold identification. *Pattern Recognition*, 39(10):1876–1891, 2006.
- [24] Stephane Lafon and Ann B Lee. Diffusion maps and coarse-graining: A unified framework for dimensionality reduction, graph partitioning, and data set parameterization. *IEEE transactions on pattern analysis and machine intelligence*, 28(9):1393–1403, 2006.
- [25] Ren-Cang Li. Relative perturbation theory:(ii) eigenspace variations. Technical report, 1994.
- [26] Oren E Livne and Achi Brandt. Lean algebraic multigrid (lamg): Fast graph laplacian linear solver. *SIAM Journal on Scientific Computing*, 34(4):B499–B522, 2012.
- [27] Andreas Loukas and Pierre Vandergheynst. Spectrally approximating large graphs with smaller graphs. In *International Conference on Machine Learning (ICML)*, 2018.
- [28] Lionel Martin, Andreas Loukas, and Pierre Vandergheynst. Fast approximate spectral clustering for dynamic networks. In *International Conference on Machine Learning (ICML)*, 2018.
- [29] Robert Preis and Ralf Diekmann. Party-a software library for graph partitioning. *Advances in Computational Mechanics with Parallel and Distributed Processing*, pages 63–71, 1997.
- [30] Dorit Ron, Ilya Safro, and Achi Brandt. Relaxation-based coarsening and multiscale graph organization. *Multiscale Modeling & Simulation*, 9(1):407–423, 2011.
- [31] Ilya Safro, Peter Sanders, and Christian Schulz. Advanced coarsening schemes for graph partitioning. *Journal of Experimental Algorithmics (JEA)*, 19:2–2, 2015.
- [32] David I Shuman, Mohammad Javad Faraji, and Pierre Vandergheynst. A multiscale pyramid transform for graph signals. *IEEE Transactions on Signal Processing*, 64(8):2119–2134, 2016.
- [33] Martin Simonovsky and Nikos Komodakis. Dynamic edge-conditioned filters in convolutional neural networks on graphs. In *IEEE Conference on Computer Vision and Pattern Recognition (CVPR)*, 2017.
- [34] Daniel A Spielman and Shang-Hua Teng. Spectral sparsification of graphs. *SIAM Journal on Computing*, 40(4):981–1025, 2011.
- [35] Gilbert W Stewart. Matrix perturbation theory. 1990.
- [36] Greg Turk and Marc Levoy. Zippered polygon meshes from range images. In *Proceedings of the 21st annual conference on Computer graphics and interactive techniques*, pages 311–318. ACM, 1994.
- [37] John C Urschel, Xiaozhe Hu, Jinchao Xu, and Ludmil T Zikatanov. A cascadic multigrid algorithm for computing the fiedler vector of graph laplacians. *arXiv preprint arXiv:1412.0565*, 2014.
- [38] Chris Walshaw. A multilevel algorithm for force-directed graph drawing. In *International Symposium on Graph Drawing*, pages 171–182. Springer, 2000.
- [39] Chris Walshaw. A multilevel algorithm for force-directed graph-drawing. *Journal of Graph Algorithms and Applications*, 7(3):253–285, 2006.

- [40] Lu Wang, Yanghua Xiao, Bin Shao, and Haixun Wang. How to partition a billion-node graph. In *Data Engineering (ICDE), 2014 IEEE 30th International Conference on*, pages 568–579. IEEE, 2014.
- [41] Richard C Wilson and Ping Zhu. A study of graph spectra for comparing graphs and trees. *Pattern Recognition*, 41(9):2833–2841, 2008.

## A Deferred proofs

### A.1 Proof of Property 2.1

We draw up an inductive argument demonstrating that  $\Pi$  is a projection matrix. The *base case*, i.e., that  $A_c = P_c^+ P_c$  is a projection matrix follows by the definition of the pseudo-inverse:  $A_c A_c = P_c^+ P_c P_c^+ P_c = P_c^+ P_c = A_c$ , where we used the property  $P_c = P_c P_c^+ P_c$ .

For the *inductive step*, we argue that if  $A_{\ell+1}$  is a projection matrix the same holds for

$$A_\ell = P_\ell^+ A_{\ell+1} P_\ell.$$

To this end, let  $P_\ell = U \Sigma V^\top$  be the singular-value decomposition with  $\Sigma = (D; 0) \in \mathbb{R}^{N_{\ell+1} \times N_\ell}$  decomposed into the  $N_{\ell+1} \times N_{\ell+1}$  diagonal matrix  $D$  and the all zero matrix 0. Then

$$A_\ell = V \Sigma^+ U^\top A_{\ell+1} U \Sigma V^\top.$$

Recalling that a projection matrix remains projective if it undergoes a similarity transformation, we deduce that  $U^\top A_{\ell+1} U$  is also projective and, moreover, if  $\Sigma^+ U^\top A_{\ell+1} U \Sigma$  is a projection matrix, so is  $A_\ell$ . The latter matrix can be written as

$$\Sigma^+ U^\top A_{\ell+1} U \Sigma = \begin{pmatrix} D^{-1} & 0 \\ 0 & 0 \end{pmatrix} U^\top A_{\ell+1} U \begin{pmatrix} D & 0 \\ 0 & 0 \end{pmatrix} = \begin{pmatrix} D^{-1} U^\top A_{\ell+1} U D & 0 \\ 0 & 0 \end{pmatrix}.$$

As a block diagonal matrix whose blocks are projective (again  $D^{-1} U^\top A_{\ell+1} U D$  is a similarity transformation),  $\Sigma^+ U^\top A_{\ell+1} U \Sigma$  is also a projection matrix. The proof that  $\Pi$  is a projection matrix concludes by letting the induction unfold backwards from  $c$  to 1 and setting  $\Pi = A_1$ .

### A.2 Proof of Lemma 2.5

For notational convenience, we drop the level index supposing that  $c = 1$  and thus  $P$  is an  $n \times N$  coarsening matrix. As we will see in the following,  $P$  has rank  $n$  and thus to prove that  $P^+ = P^\top D^{-2}$ , it is sufficient to show that matrix  $\Pi = P^\top D^{-2} P$  is a projection matrix of rank  $n$  (and thus equal to  $P^+ P$ ). Matrix  $\tilde{P} = D^{-1} P$  has the same sparsity structure as  $P$  and is thus also a coarsening matrix. W.l.o.g. let the rows of  $P$  be sorted based on their support, such that for any two rows  $r < r'$  and  $P(r, i), P(r', i') \neq 0$  we necessarily have  $i < i'$ . Furthermore, denote by  $p_r$  the vector containing all non-zero entries of  $P(r, :)$  such that  $\|p_r\|_2 = \|P(r, :)\|_2 = D(r, r)$ . Due to the disjoint support of the rows of  $P$  and under this particular sorting, matrix  $\Pi$  is block-diagonal. Moreover, each block  $B_r$  in its diagonal is a rank 1 projection matrix as  $B_r^2 = B_r B_r = (p_r D(r, r)^{-2} p_r^\top) (p_r D(r, r)^{-2} p_r^\top) = p_r D(r, r)^{-2} p_r^\top \frac{p_r^\top p_r}{\|p_r\|_2^2} = B_r$ . We have thus arrived to the relation  $\Pi^2 = \Pi$ , which constitutes a necessary and sufficient condition for  $\Pi$  to be a projection matrix. The block-diagonal structure of  $\Pi$  also implies that its rank (as well as that of  $P$ ) is  $n$ .

### A.3 Proof of Lemma 2.6

Let us first remark that, by Lemma 2.5,  $A = P^\mp$  is also a coarsening matrix with the same sparsity structure as  $P$ .

*Necessity.* We start by considering the nullspace of  $L_c = ALA^\top$  and aim to ensure that it is equal to the span of the constant vector 1, which is a necessity for all combinatorial Laplacian matrices. Since matrix  $A$  is full row-rank and  $L$  has rank  $N - 1$ , the nullspace of  $L_c$  is one dimensional. Therefore, the nullspace is correct as long as  $1^\top ALA^\top 1 = 0$ , which happens if either  $A^\top 1 = \alpha 1$  for a constant  $\alpha$  or  $A^\top 1 = 0$ . In both cases,  $(A^\top 1)(r) = \alpha 1$  for every  $r$ . By the definition of  $A$  however we know that its rows have disjoint support and, as such, vector  $A^\top 1$  exactly contains the non-zero entries of  $A$ . In other words, for the nullspace of  $L_c$  to be properly formed, the non-zero entries of  $A$  should either all be equal to  $\alpha$  (such that  $A^\top 1 = \alpha 1$ ) or zero (in which case  $A^\top 1 = 0$ ). The latter case can clearly be discarded as it would disconnect the graph. We have thus discovered that  $ALA^\top$  has a properly formed nullspace if and only if the non-zero entries of  $A$  are equal, rendering the latter condition necessary.

*Sufficiency.* Considering that every Laplacian of  $M$  edges can be re-written as  $L = S^\top S$ , where  $S$  is the  $M \times N$  incidence matrix, we can confirm that our condition is also sufficient by showing that, for every  $A$  with equal non-zero entries, the matrix  $S_c = SA^\top$  is an incidence matrix of  $L_c$  such that  $L_c = S_c^\top S_c$ . W.l.o.g., suppose that  $\alpha = 1$  ( $\alpha^2 L$  is a valid Laplacian for all  $\alpha$ ). By construction, each row of  $S_c$  is  $S_c(q, :)^\top = AS(q, :)^\top$ . Name as  $e_{ij}$  the corresponding edge, such that  $S(q, :)^\top = \delta_i - \delta_j$ , where  $\delta_i$  is a dirac centered at vertex  $v_i$ . We have that  $S_c(q, :)^\top = A\delta_i - A\delta_j$ . Obviously, if none of  $v_i, v_j$  are coarsened then  $S_c(q, :)^\top = \delta_i - \delta_j$ , which is a valid row. Moreover, by construction of  $A$ , if either of  $v_i, v_j$  is coarsened (but not both) or if  $v_i, v_j$  are coarsened into different vertices then both relations  $A\delta_i = \delta_i$  and  $A\delta_j = \delta_j$  hold and thus once more  $S_c(q, :)^\top = \delta_i - \delta_j$  is a valid row. Lastly, if  $v_i, v_j$  are coarsened into the same vertex then for some  $r$  it must be that  $A(r, i) = A(r, j)$ , whereas  $A(r', i) = A(r', j) = 0$  for all  $r' \neq r$  and thus  $S_c(r, :)^\top = 0$ , signifying that the edge is not present. Summarizing, in every case  $S_c$  is a valid incidence matrix, rendering our condition also sufficient.

### A.4 Proof of Theorem 2.3

The Courant-Fischer min-max theorem for a hermitian matrix  $L$  reads

$$\lambda_k = \min_{\dim(\mathcal{U})=k} \max_{x \in \text{span}(\mathcal{U})} \left\{ \frac{x^\top L x}{x^\top x} \mid x \neq 0 \right\}, \quad (9)$$

whereas the same theorem for  $L_c$  gives

$$\begin{aligned} \tilde{\lambda}_k &= \min_{\dim(\mathcal{U}_c)=k} \max_{x_c \in \text{span}(\mathcal{U}_c)} \left\{ \frac{x_c^\top L_c x_c}{x_c^\top x_c} \mid x_c \neq 0 \right\} = \min_{\dim(\mathcal{U}_c)=k} \max_{Px \in \text{span}(\mathcal{U}_c)} \left\{ \frac{x^\top \Pi L \Pi x}{x^\top \Pi x} \mid x \neq 0 \right\} \\ &= \min_{\dim(\mathcal{U})=k, \mathcal{U} \subseteq \text{im}(\Pi)} \max_{x \in \text{span}(\mathcal{U})} \left\{ \frac{x^\top L x}{x^\top x} \mid x \neq 0 \right\}, \end{aligned}$$

where in the second equality we set  $L_c = P^\mp L P^+$  and  $x_c = Px$  and the third equality holds since  $\Pi$  is a projection matrix (see Property 2.1). Notice how, with the exception of the constraint that  $x = \Pi x$ , the final optimization problem is identical to the one for  $\lambda_k$ , given in (9). As such, the former's solution must be strictly larger (since it is a more constrained problem) and we have that  $\tilde{\lambda}_k \geq \lambda_k$ .

Analogously, one obtains the lower inequality  $\tilde{\lambda}_{k-(N-n)} \leq \lambda_k$  by applying the same argument on matrices  $-L$  and  $-L_c$  and exploiting that the  $k$ -th largest eigenvalue of any matrix  $M$  is also the  $k$ -th smallest eigenvalue of  $-M$ .

## A.5 Proof of Theorem 3.2

We start by proving that, for any integer  $k \leq n$  and for all  $x \in \text{span}(V)$  the inequality

$$(1 - \epsilon) \|x\|_L \leq \|x_c\|_{L_c} \leq (1 + \epsilon) \|x\|_L$$

holds as long as  $\epsilon = \|\Pi^\perp B_0\|_L$  is smaller than 1, where  $B_0 = VV^\top L^{+1/2}$ . We remind the reader that  $\|x\|_L = \|Sx\|_2$  and  $\|x\|_{L_c} = \|S\Pi x\|_2$ . For our upper bound, we then derive:

$$\begin{aligned} \max_{x \in \text{span}(V)} \frac{\|S\Pi x\|_2 - \|Sx\|_2}{\|Sx\|_2} &\leq \max_{x \in \text{span}(V)} \frac{\|Sx\|_2 + \|\Pi^\perp x\|_2 - \|Sx\|_2}{\|Sx\|_2} \\ &= \max_{a \in \mathbb{R}^k} \frac{\|\Pi^\perp Va\|_2}{\|L^{1/2}Va\|_2} = \max_{b \in \mathbb{R}^N} \frac{\|\Pi^\perp VV^\top L^{+1/2}b\|_2}{\|b\|_2} = \|\Pi^\perp VV^\top L^{+1/2}\|_2 = \epsilon. \end{aligned}$$

Similarly, whenever  $\|Sx\|_2 \geq \|\Pi^\perp x\|_2$  we can write

$$\begin{aligned} \min_{x \in \text{span}(V)} \frac{\|S\Pi x\|_2 - \|Sx\|_2}{\|Sx\|_2} &\geq \min_{x \in \text{span}(V)} \frac{\|Sx\|_2 - \|\Pi^\perp x\|_2 - \|Sx\|_2}{\|Sx\|_2} \\ &= - \max_{a \in \mathbb{R}^k} \frac{\|\Pi^\perp Va\|_2}{\|L^{1/2}Va\|_2} = -\|\Pi^\perp VV^\top L^{+1/2}\|_2 = -\epsilon. \end{aligned}$$

Considering the unitary invariance of the spectral norm, the above inequalities imply the claimed result.

In addition, as the following technical Lemma claims, in a multilevel scheme, any  $\|\Pi^\perp x\|_L$  can be broken down into the contributions of each level:

**Lemma A.1.** *Define projection matrices  $\Pi_\ell = P_\ell^+ P_\ell$  and  $\Pi_\ell^\perp = I - \Pi_\ell$ . If*

$$\|\Pi_\ell^\perp x_{\ell-1}\|_{L_{\ell-1}} \leq \epsilon_\ell \|x_{\ell-1}\|_{L_{\ell-1}} \quad \text{at each level } \ell \leq c,$$

*then the multilevel error is bounded by*

$$\|\Pi^\perp x\|_L \leq \left( \sum_{\ell=1}^c \epsilon_\ell \prod_{q=1}^{\ell-1} (1 + \epsilon_q) \right) \|x\|_L.$$

*Proof.* We recursively apply the following inequality

$$\begin{aligned} \|S_{\ell-1} \Pi_\ell^\perp x_{\ell-1}\|_2 &\leq \epsilon_\ell \|S_{\ell-1} x_{\ell-1}\|_2 \\ &= \epsilon_\ell \|S_{\ell-2} \Pi_{\ell-1} x_{\ell-2}\|_2 \\ &\leq \epsilon_\ell (\|S_{\ell-2} x_{\ell-2}\|_2 + \|S_{\ell-2} \Pi_{\ell-1}^\perp x_{\ell-2}\|_2) \\ &\leq \epsilon_\ell (\|S_{\ell-2} x_{\ell-2}\|_2 + \epsilon_{\ell-1} \|S_{\ell-2} x_{\ell-2}\|_2) = \epsilon_\ell (1 + \epsilon_{\ell-1}) \|S_{\ell-2} x_{\ell-2}\|_2 \end{aligned}$$

to deduce that

$$\|S_{\ell-1} \Pi_\ell^\perp x_{\ell-1}\|_2 \leq \epsilon_\ell \prod_{q=1}^{\ell-1} (1 + \epsilon_q) \|S_0 x_0\|_2 = \epsilon_\ell \prod_{q=1}^{\ell-1} (1 + \epsilon_q) \|x\|_L.$$

We control the end-to-end error  $\|S\Pi^\perp x\|_2$  with a simple telescopic series argument.

$$\begin{aligned}\|\Pi^\perp x\|_L &= \|S_0\Pi^\perp x_0\|_2 = \|S_0x_0 - S_c x_c\|_2 \\ &\leq \|S_0x_0 - S_1x_1\|_2 + \|S_1x_1 - S_2x_2\|_2 + \dots + \|S_{c-1}x_{c-1} - S_c x_c\|_2 \\ &= \|S_0\Pi_1^\perp x_1\|_2 + \|S_1\Pi_1^\perp x_1\|_2 + \dots + \|S_{c-1}\Pi_1^\perp x_{c-1}\|_2\end{aligned}$$

Together, the above two results imply the desired bound.  $\square$

Therefore, to guarantee that in a multilevel scheme

$$\|\Pi^\perp B_0\|_L = \max_{b \in \mathbb{R}^N} \frac{\|S\Pi^\perp B_0 b\|_2}{\|b\|_2} \leq \epsilon,$$

one needs to make sure that, for each level  $\ell = 1, \dots, c$ , the following holds:

$$\frac{\|S_{\ell-1}\Pi_\ell^\perp x_{\ell-1}\|_2}{\|S_{\ell-1}x_{\ell-1}\|_2} \leq \epsilon_\ell, \quad \text{for all } x_{\ell-1} = P_{\ell-1} \cdots P_1 B_0 b$$

By the same argument used for the multilevel error, when  $\ell = 1$ , we have that  $\epsilon_1 = \|\Pi_1^\perp B_0\|_{L_0}$ . For all other  $\ell$ , set  $B_{\ell-1} = P_{\ell-1} \cdots P_1 B_0$  and further let  $(B_{\ell-1}^\top L_{\ell-1} B_{\ell-1})^{+1/2}$  be the pseudo-inverse of the matrix square-root of the  $N \times N$  matrix  $B_{\ell-1}^\top L_{\ell-1} B_{\ell-1}$ . By the substitution  $b = S_{\ell-1}B_{\ell-1}a$ , we can rewrite the above as

$$\max_{b \in \mathbb{R}^N} \frac{\|S_{\ell-1}\Pi_\ell^\perp B_{\ell-1}b\|_2}{\|S_{\ell-1}B_{\ell-1}b\|_2} = \max_{b \in \mathbb{R}^N} \frac{\|S_{\ell-1}\Pi_\ell^\perp B_{\ell-1}(B_{\ell-1}^\top L_{\ell-1} B_{\ell-1})^{+1/2}b\|_2}{\|b\|_2}.$$

For  $\ell > 1$ , therefore  $\epsilon_\ell = \|\Pi_\ell^\perp A_{\ell-1}\|_{L_{\ell-1}}$  with  $A_{\ell-1} = B_{\ell-1}(B_{\ell-1}^\top L_{\ell-1} B_{\ell-1})^{+1/2}$ .

## A.6 Proof of Theorem 3.3

The lower bound is given by Theorem 2.3. For the upper bound, we adopt a variational approach and reason that, since

$$\tilde{\lambda}_k = \min_{\dim(U_c)=k} \max_{x_c \in \text{span}(U_c)} \left\{ \frac{x_c^\top L_c x_c}{x_c^\top x_c} \mid x_c \neq 0 \right\} = \min_{\dim(U)=k} \max_{x \in \text{span}(U)} \left\{ \frac{x^\top \Pi L \Pi x}{x^\top \Pi x} \mid x \neq 0 \right\},$$

for any matrix  $V$  the following inequality holds:

$$\tilde{\lambda}_k \leq \max_{x \in \text{span}(V)} \left\{ \frac{x^\top \Pi L \Pi x}{x^\top \Pi x} \mid x \neq 0 \right\},$$

as long as the columnspace of  $V$  is of dimension  $k$  and does not coincide with the nullspace of  $\Pi$ . We consider  $V = U_k$  for which

$$\tilde{\lambda}_k \leq \max_{x \in \text{span}(U_k)} \left\{ \frac{x^\top \Pi L \Pi x}{x^\top \Pi x} \mid x \neq 0 \right\} = \max_{x \in \text{span}(U_k)} \left\{ \frac{\|S\Pi x\|_2^2}{\|\Pi x\|_2^2} \mid x \neq 0 \right\}.$$

It will be convenient to manipulate the square-root of this quantity:

$$\sqrt{\tilde{\lambda}_k} \leq \max_{a \in \mathbb{R}^k} \frac{\|S\Pi U_k a\|_2}{\|\Pi U_k a\|_2} \leq \frac{\|S\Pi U_k\|_2}{\|\Pi U_k\|_2} \leq \frac{\|S U_k\|_2 + \|S\Pi^\perp U_k\|_2}{\|\Pi U_k\|_2} = \frac{\sqrt{\lambda_k} + \|S\Pi^\perp U_k\|_2}{\|\Pi U_k\|_2}.$$

The norm in the numerator is upper bounded by

$$\begin{aligned}\|S\Pi^\perp U_k\|_2 &= \|S\Pi^\perp U_k \Lambda_k^{-1/2} \Lambda_k^{1/2}\|_2 \leq \|S\Pi^\perp U_k \Lambda_k^{-1/2}\|_2 \|\Lambda_k^{1/2}\|_2 \\ &= \sqrt{\lambda_k} \|S\Pi^\perp U_k \Lambda_k^{-1/2}\|_2 = \sqrt{\lambda_k} \epsilon_k.\end{aligned}$$

The final inequality then follows directly by taking the square and noticing that, since  $\Pi$  is a projection matrix, the denominator can be re-written as  $\|\Pi U_k\|_2^2 = 1 - \|\Pi^\perp U_k\|_2^2$ .

## A.7 Proof of Theorem 3.4

Li [25] showed that we can express the  $\sin\Theta$  as a sum of squared inner products  $(\tilde{u}_j^\top P u_i)^2$ :

$$\left\| \sin\Theta(U_k, P^\top \tilde{U}_k) \right\|_F^2 = \left\| \tilde{U}_{k^\perp}^\top P U_k \right\|_F^2 = \sum_{i \leq k} \sum_{j > k} (\tilde{u}_j^\top P u_i)^2 \quad (10)$$

If  $L_c$  and  $L$  are  $(\mathcal{U}_i, \epsilon_i)$ -similar we have that

$$(1 - \epsilon_i)^2 \lambda_i \leq u_i^\top P^\top L_c P u_i \leq (1 + \epsilon_i)^2 \lambda_i$$

and this is true as long as  $\epsilon_i \leq 1$ . Summing these inequalities for all  $i \leq k$  amounts to

$$\sum_{i \leq k} (1 + \epsilon_i)^2 \lambda_i \geq \sum_{i \leq k} \sum_{j=1}^n \tilde{\lambda}_j (\tilde{u}_j^\top P u_i)^2 = \sum_{j \leq k} \tilde{\lambda}_j \sum_{i \leq k} (\tilde{u}_j^\top P u_i)^2 + \sum_{j > k} \tilde{\lambda}_j \sum_{i \leq k} (\tilde{u}_j^\top P u_i)^2. \quad (11)$$

We perform the following manipulation

$$\begin{aligned}\sum_{j \leq k} \tilde{\lambda}_j \sum_{i \leq k} (\tilde{u}_j^\top P u_i)^2 &\geq \sum_{j \leq k} \lambda_j \sum_{i \leq k} (\tilde{u}_j^\top P u_i)^2 = \sum_{j \leq k} \lambda_j \left( 1 - \sum_{i > k} (\tilde{u}_j^\top P u_i)^2 \right) \\ &\geq \sum_{j \leq k} \lambda_j - \lambda_k \sum_{i \leq k} \left( \|\Pi^\perp u_i\|_2^2 + \sum_{j \geq k} (\tilde{u}_j^\top P u_i)^2 \right),\end{aligned}$$

which together with (10) and (11) yields

$$\left\| \sin\Theta(U_k, P^\top \tilde{U}_k) \right\|_F^2 \leq \sum_{i \leq k} \frac{(1 + \epsilon_i)^2 \lambda_i - \lambda_i + \lambda_k \|\Pi^\perp u_i\|_2^2}{\tilde{\lambda}_{k+1} - \lambda_k} = \sum_{i=1}^k \frac{\epsilon_i (2 + \epsilon_i) \lambda_i + \lambda_k \|\Pi^\perp u_i\|_2^2}{\tilde{\lambda}_{k+1} - \lambda_k},$$

which, after noting that  $\epsilon_i \leq \epsilon_k$ , becomes the desired inequality.

## A.8 Proof of Corollary 3.5

The lower bound is a direct consequence of coarsening: for any set  $S_c \subset \mathcal{V}_c$  define the vertex set  $S \subset \mathcal{V}$  such that  $v_i \in S$  if and only if  $\varphi(v_i) \in S_c$ . Clearly,  $|S| \geq |S_c|$ . In addition, by the definition of consistent coarsening and since every contraction set belongs either in  $S$  or  $S_c$  (but not in both), we have that  $e(S, \bar{S}) = e(S_c, \bar{S}_c)$ . In other words, for every  $S_c$  there exists an  $S$  such that  $\frac{e(S, \bar{S})}{|S|} \leq \frac{e(S_c, \bar{S}_c)}{|S_c|}$ , implying  $i(G) \leq i(G_c)$  as desired.

For the upper bound, we combine the isoperimetric inequality  $\frac{\lambda_2}{2} \leq i(G) \leq \sqrt{2d_{\max}(G) \lambda_2}$  with Theorem 3.3 and write

$$i(G_c) \leq \sqrt{2d_{\max} \tilde{\lambda}_2} \leq \frac{(1 + \epsilon)}{\|\Pi u_2\|_2} \sqrt{2d_{\max} \lambda_2} \leq 2 \frac{(1 + \epsilon)}{\|\Pi u_2\|_2} \sqrt{d_{\max}(G_c) i(G)},$$

which completes our proof.

## A.9 Proof of Theorem 4.1

For notational simplicity in the context of this proof we drop level indices and assume that only a single coarsening level is used. Nevertheless, it should be stressed that this without loss of generality, as an identical argument holds for every level of our scheme.

Consider any  $x$  and set  $y = \Pi^\perp x$ . Furthermore, define for each contraction set the (i) *internal* edge set  $\mathcal{E}^{(r)} = \{e_{ij} | v_i, v_j \in \mathcal{V}^{(r)} \text{ and } e_{ij} \in \mathcal{E}_{\ell-1}\}$ , and (ii) the *boundary* edge set  $\partial\mathcal{E}^{(r)}$ , such that if  $e_{ij} \in \partial\mathcal{E}^{(r)}$  then  $v_i \in \mathcal{V}^{(r)}$  and  $v_j \notin \mathcal{V}^{(r)}$ . We have that

$$\begin{aligned} \|\Pi^\perp x\|_L^2 &= \sum_{e_{ij} \in \mathcal{E}} w_{ij}(y(i) - y(j))^2 \\ &= \sum_{r=1}^n \left( \underbrace{\sum_{e_{ij} \in \mathcal{E}^{(r)}} w_{ij}(y(i) - y(j))^2}_{a_r} + \underbrace{\frac{1}{2} \sum_{e_{ij} \in \partial\mathcal{E}^{(r)}} w_{ij}(y(i) - y(j))^2}_{b_r} \right). \end{aligned}$$

In the following, we will express  $a_r$  and  $b_r$  as a function of the vector  $y_r = \Pi_{\mathcal{V}^{(r)}}^\perp x$ . Term  $a_r$  is luckily independent of any other contraction set:

$$a_r = \sum_{e_{ij} \in \mathcal{E}^{(r)}} w_{ij}(y(i) - y(j))^2 = \sum_{e_{ij} \in \mathcal{E}^{(r)}} w_{ij}(y_r(i) - y_r(j))^2.$$

On the other hand,  $b_r$  is smaller than

$$b_r = \sum_{e_{ij} \in \partial\mathcal{E}^{(r)}} w_{ij}(y(i) - y(j))^2 \leq 2 \sum_{e_{ij} \in \partial\mathcal{E}^{(r)}} w_{ij}(y(i) - 0)^2 + 2 \sum_{e_{ij} \in \partial\mathcal{E}^{(r)}} w_{ij}(0 - y(j))^2.$$

Distributing the second quantities, respectively, amongst the contraction sets that include said vertices, we get

$$\begin{aligned} \|\Pi^\perp x\|_L^2 &\leq \sum_{r=1}^n \left( \sum_{e_{ij} \in \mathcal{E}^{(r)}} w_{ij}(y_r(i) - y_r(j))^2 + 2 \sum_{e_{ij} \in \partial\mathcal{E}^{(r)}} w_{ij}(y(i) - 0)^2 \right) \\ &= \sum_{r=1}^n \left( \sum_{e_{ij} \in \mathcal{E}^{(r)}} w_{ij}(y_r(i) - y_r(j))^2 + \sum_{e_{ij} \in \partial\mathcal{E}^{(r)}} (2w_{ij})(y_r(i) - y_r(j))^2 \right) \\ &= \sum_{r=1}^n \|y_r\|_{L_{\mathcal{V}^{(r)}}}^2 = \sum_{\mathcal{C} \in \mathcal{P}} \|y_r\|_{L_{\mathcal{C}}}^2. \end{aligned}$$

Above, in the second step we used the fact that  $[\Pi^\perp](i) = 0$  for all  $v_i \notin \mathcal{C}$ . A “decoupled” bound can then be obtained as follows:

$$\|\Pi^\perp A\|_L^2 = \max_{a \in \mathbb{R}^{k-1}} \frac{\|S\Pi^\perp A a\|_2^2}{\|a\|_2^2} \leq \sum_{\mathcal{C} \in \mathcal{P}} \max_{a \in \mathbb{R}^{k-1}} \frac{\|\Pi_{\mathcal{C}}^\perp A a\|_{L_{\mathcal{C}}}^2}{\|a\|_2^2} = \sum_{\mathcal{C} \in \mathcal{P}} \|\Pi_{\mathcal{C}}^\perp A\|_{L_{\mathcal{C}}}^2$$

The final inequality is derived by taking the square-root of the last equation.

## B Complexity analysis

The computational complexity of Algorithm 1 depends on the number of nodes  $N$  and edges  $M$  of our graph, the number of levels  $c$ , the subspace size  $k$ , as well as on how the families of candidate

sets are formed. To derive worst-case bounds, we denote by  $\Phi_\ell = \sum_{\mathcal{C} \in \mathcal{F}_\ell} |\mathcal{C}|$  the number of vertices in all candidate sets and by  $\delta = \max_{\ell, \mathcal{C} \in \mathcal{F}_\ell} |\mathcal{C}|$  the cardinality of the maximum candidate set over all levels. Furthermore, we suppose that the per-level reduction ratio  $r_\ell$  is a constant.

We start with some basic observations:

- *Computing  $A_0, \dots, A_{c-1}$  is possible in  $O(ckM + k^2N + ck^3)$  operations when  $V = U_k$ .* Each  $A_{\ell-1}$  is computed once for each level. For  $\ell = 1$ , we need to approximate the first  $k$  eigenpairs of  $L$ , which can be achieved in  $O(kM)$  operations using the Lanczos method. For consecutive levels, forming matrix  $B_{\ell-1}^\top L_{\ell-1} B_{\ell-1}$  takes  $O(M_{\ell-1}k + N_{\ell-1}k^2)$  operations, whereas computing the pseudo-square-root  $(B_{\ell-1}^\top L_{\ell-1} B_{\ell-1})^{+1/2}$  is possible in  $O(k^3)$  operations. Summing up the costs for all levels, we get  $O(k \sum_{\ell=1}^c M_{\ell-1} + k^2 \sum_{\ell=2}^c N_{\ell-1} + ck^3) = O(ckM + k^2N + ck^3)$ , where we used the observation that  $\sum_{\ell=2}^c N_{\ell-1} = O(N)$ .
- *At each level, the cost function is evaluated at most  $\Phi_\ell$  times.* One starts by computing the cost of each candidate set in  $\mathcal{F}_\ell$ . Moreover, every  $\mathcal{C}$  added to  $\mathcal{P}_\ell$  causes the pruning of at most  $\sum_{v_i \in \mathcal{C}} (\phi_i - 1)$  other sets, where  $\phi_i$  is the number of candidate sets that include  $v_i$ . Since  $\mathcal{P}_\ell$  is a partitioning of  $\mathcal{V}_{\ell-1}$ , at most  $\sum_{\mathcal{C} \in \mathcal{P}_\ell} \sum_{v_i \in \mathcal{C}} (\phi_i - 1) \leq \sum_{v_i \in \mathcal{V}_{\ell-1}} \phi_i - |\mathcal{F}_\ell| = \Phi_\ell - |\mathcal{F}_\ell|$  cost re-evaluation are needed.
- *Given  $A_{\ell-1}$ , each call of  $\text{cost}_\ell(\mathcal{C})$  requires  $O(\min\{k^2\delta + k\delta^2, k\delta^2 + \delta^3\})$  operations.* The involved matrices themselves can be easily formed since, excluding all-zero rows and columns, both  $L_{\mathcal{C}}$  and  $\Pi_{\mathcal{C}}^\perp$  are  $|\mathcal{C}| \times |\mathcal{C}|$  matrices and we can safely restrict  $A_{\ell-1}$  to be of size  $|\mathcal{C}| \times k$  by deleting all rows that would have been multiplied by zero. Now, by definition, the incidence matrix  $S_{\mathcal{C}}$  of  $L_{\mathcal{C}}$  has at most  $\delta$  columns and  $2\delta$  rows (since we can bundle all boundary weights of a vertex in  $\mathcal{C}$  in a single row). Depending on the relative size of  $k$  and  $\delta$  we can perform the computation in two ways:
  - Either we form the  $k \times k$  matrix  $A_{\ell-1}^\top \Pi_{\mathcal{C}}^\perp L_{\mathcal{C}} \Pi_{\mathcal{C}}^\perp A_{\ell-1}$  and approximate its spectral norm paying a total of  $O(k^2\delta + k\delta^2)$ .
  - Otherwise, we form the  $2d \times 2d$  matrix  $S_{\mathcal{C}} \Pi_{\mathcal{C}}^\perp A_{\ell-1} A_{\ell-1}^\top \Pi_{\mathcal{C}}^\perp S_{\mathcal{C}}^\top$  and compute its norm at a combined cost of  $O(\delta^2k + \delta^3)$ .
- *Maintaining  $\mathcal{F}_\ell$  sorted incurs  $O(\Phi_\ell \log |\mathcal{F}_\ell|)$  cost.* Sorting  $\mathcal{F}_\ell$  during initialization entails  $O(|\mathcal{F}_\ell| \log |\mathcal{F}_\ell|)$  operations. Inserting each  $\mathcal{C}'$  into  $\mathcal{F}_\ell$  (see step 11) can be done in  $O(\log |\mathcal{F}_\ell|)$  and, moreover, by the same argument used to bound the number of cost evaluations, at most  $\Phi_\ell - |\mathcal{F}_\ell|$  such insertions can happen.
- *Other operations carry negligible cost.* In particular, by implementing `marked` as a binary array, checking if a vertex is marked or not can be done in constant time.

Overall, using Algorithm 1 and for  $\mathcal{R} = \mathcal{U}_k$  we can coarsen a graph in  $O(ckM + k^2N + ck^3 + \sum_{\ell=1}^c \Phi_\ell (\min\{k^2\delta + k\delta^2, k\delta^2 + \delta^3\} + \log |\mathcal{F}_\ell|))$  operations.

**Acknowledgements.** This work was kindly supported by the Swiss National Science Foundation (SNSF) in the context of the project “Deep Learning for Graph-structured Data”. I would also like to thank Rodrigo Cerqueira Gonzalez Pena and Defferrard Michaël for their useful comments.